Different molecular changes underlie the same phenotypic transition: origins and consequences of independent shifts to homostyly within species

Emiliano Mora-Carrera[1], Rebecca Stubbs[1], Barbara Keller[1], Étienne Léveillé-Bourret [1], Jurriaan de Vos[2], Peter Szövényi[1], and Elena Conti[1]

[1]University of Zurich
[2]University of Basel

June 21, 2021

Abstract

The repeated transition from outcrossing to selfing is a key topic in evolutionary biology. However, the molecular basis of such shifts has been rarely examined due to lack of knowledge of the genes controlling these transitions. A classic example of mating system transition is the repeated shift from heterostyly to homostyly. Occurring in 28 angiosperm families, heterostyly is characterized by the reciprocal position of male and female sexual organs in two (or three) distinct, usually self-incompatible floral morphs. Conversely, homostyly is characterized by a single, self-compatible floral morph with reduced separation of male and female organs, facilitating selfing. Here, we investigate the origins of homostyly in *Primula vulgaris* and its microevolutionary consequences by integrating surveys of the frequency of homostyles in natural populations, DNA sequence analyses of the gene controlling the position of female sexual organs (*CYP?*), and microsatellite genotyping of both progeny arrays and natural populations characterized by varying frequencies of homostyles. As expected, we found that homostyles displace short-styled individuals, but long-style morphs are maintained at low frequencies within populations. We also demonstrated that homostyles repeatedly evolved from short-styled individuals in association with different types of loss-of-function mutations in *CYP?*. Additionally, homostyly triggers a shift to selfing, promoting increased inbreeding within and genetic differentiation among populations. Our results elucidate the causes and consequences of repeated transitions to homostyly within species, enabling a likely explanation for the fact that homostyly has not become fixed in *P. vulgaris*. This study represents a benchmark for future analyses of losses of heterostyly.

Article type: Original Article

Different molecular changes underlie the same phenotypic transition: origins and consequences of independent shifts to homostyly within species

Short title: Independent shifts to homostyly within species

Mora-Carrera E[1*], Stubbs RL[1], Keller B[1], Leveille-Bourret E[1,2], de Vos JM[3], Szövényi P[1] and Conti E[1*]

[1]Department of Systematic and Evolutionary Botany, University of Zurich, Zollikerstrasse 107, Zurich 8008, Switzerland;[2]Institut de recherche en biologie végétale, Département de sciences biologiques, Université de Montréal, Québec, Canada;

[3]Department of Environmental Sciences – Botany, University of Basel, Schönbeinstrasse 6, 4056 Basel, Switzerland;

*Corresponding authors:*emiliano.mora@systbot.uzh.ch*,*elena.conti@systbot.uzh.ch*

ABSTRACT

The repeated transition from outcrossing to selfing is a key topic in evolutionary biology. However, the molecular basis of such shifts has been rarely examined due to lack of knowledge of the genes controlling these transitions. A classic example of mating system transition is the repeated shift from heterostyly to homostyly. Occurring in 28 angiosperm families, heterostyly is characterized by the reciprocal position of male and female sexual organs in two (or three) distinct, usually self-incompatible floral morphs. Conversely, homostyly is characterized by a single, self-compatible floral morph with reduced separation of male and female organs, facilitating selfing. Here, we investigate the origins of homostyly in *Primula vulgaris* and its microevolutionary consequences by integrating surveys of the frequency of homostyles in natural populations, DNA sequence analyses of the gene controlling the position of female sexual organs (*CYP?*), and microsatellite genotyping of both progeny arrays and natural populations characterized by varying frequencies of homostyles. As expected, we found that homostyles displace short-styled individuals, but long-style morphs are maintained at low frequencies within populations. We also demonstrated that homostyles repeatedly evolved from short-styled individuals in association with different types of loss-of-function mutations in *CYP?*. Additionally, homostyly triggers a shift to selfing, promoting increased inbreeding within and genetic differentiation among populations. Our results elucidate the causes and consequences of repeated transitions to homostyly within species, enabling a likely explanation for the fact that homostyly has not become fixed in *P. vulgaris*. This study represents a benchmark for future analyses of losses of heterostyly.

KEYWORDS

heterostyly, intra-specific, loss-of-function mutations, mating system, *Primula,* selfing

1 INTRODUCTION

A central topic in evolutionary biology is the repeated transition from outcrossing to selfing (Cutter, 2019). A main advantage of selfers vs. outcrossers is the increase in the number of gene copies transmitted to the next generation (i.e., automatic selection advantage; Busch & Delph, 2012). Additionally, selfers can reproduce when mates or pollinators, in the case of plants, are scarce (i.e., reproductive assurance; Darwin, 1876). These advantages are counteracted by fitness reduction in selfed progeny due to inbreeding depression (Schemske & Lande, 1985). In plants, transitions to selfing are enabled by the loss of self-incompatibility (SI). The genetic basis of shifts from SI to self-compatibility (SC) has been investigated in systems where the genes responsible for self-pollen recognition have been characterized (Shimizu & Tsuchimatsu, 2015). Repeated transitions to SC *via* the inactivation of SI genes are often studied by comparing closely related species with contrasting mating systems (Vekemans, Poux, Goubet, & Castric, 2014). Although independent losses of SI have also been reported within species (Busch, Joly, & Schoen, 2011; Foxe et al., 2010; Goodwillie 1999), only a few studies have investigated the molecular basis of these losses (Chantha, Herman, Platts, Vekemans, & Schoen, 2013; Shimizu, Shimizu-Inatsugi, Tsuchimatsu, & Purugganan, 2008).

A classic model for the study of mating system transitions is the shift from heterostyly to homostyly (Barrett, 2019). Heterostyly, occurring in at least 28 angiosperm families, is a floral polymorphism that promotes outcrossing, whereby two (distyly) or three (tristyly) floral morphs differing in the position of reproductive organs co-occur in a population (Darwin, 1877). In distylous species, flowers of the long-styled morph, henceforth L-morph (also known as pin), exhibit the stigma above the anthers, whereas flowers of the short-styled morph, henceforth S-morph (also known as thrum), show the reciprocal arrangement (Ganders, 1979; Figure 1). The reciprocal position of male and female sexual organs in flowers of heterostylous taxa simultaneously promotes pollen export to individuals of the opposite floral morph and reduces self-pollination (Keller, Thomson, & Conti, 2014; Lloyd & Webb, 1992). Moreover, heterostyly is often, but not always, associated with a heteromorphic self-incompatibility system that reduces self- and intra-morph fertilization (Dulberger, 1992). Heterostyly is controlled by a single Mendelian locus known as the heterostyly supergene or S-locus (Lewis & Jones, 1992). Recent genomic and functional studies in *Primula* indicated that the S-locus is entirely absent from the L-morph and hemizygous in the S-morph, where it consists of five tightly linked genes (Huu et al., 2016; Li et al., 2016). Two genes in the S-locus, GLOBOSA2 (*GLO?*) and CYP734A50

(*CYP?*), have been experimentally demonstrated to control anther and stigma positions, respectively (Huu et al., 2016; 2020).

As common for complex traits, heterostyly has been repeatedly lost. Conforming to predictions about mating system transitions, losses of heterostyly are usually associated with the decline or absence of specialized pollinators (Pérez-Barrales & Arroyo, 2010; Yuan et al., 2017) or the absence of plant mates, as in colonization after long-distance dispersal (Ness, Wright, & Barrett, 2010) and recolonization after glacial retreat (Guggisberg, Mansion, Kelso, & Conti, 2006). The breakdown of heterostyly can occur either through the loss of one or more of the heterostylous floral morphs (e.g., transitions from tristyly and distyly to monomorphism; Ness et al., 2010; Pérez-Barrales, Pino, Albaladejo, & Arroyo, 2009) or the invasion of homostylous plants (Barrett, 2019). Homostylous flowers are characterized by reduced distance between male and female sexual organs (i.e., reduced herkogamy) and, typically, loss of SI (de Vos et al., 2014). Both long- and short-homostyles are known, the latter being rare (Lewis & Jones, 1992). Long- and short-homostyles, respectively, bear both anthers and stigmas either higher (H-morph in Figure 1) or lower in the corolla tube. Homostyly enables reproductive assurance through autonomous self-pollination, as demonstrated in *Primula* (Carlson, Gisler, & Kelso, 2008; de Vos, Keller, Isham, Kelso, & Conti, 2012; Yuan et al., 2017), and increases selfing rates (Husband & Barrett, 1993; Schoen, Johnston, L'Heureux, & Marsolais, 1997; Zhong et al., 2019). Repeated shifts from heterostyly to homostyly have been reported both between (de Vos, Hughes, Schneeweiss, Moore, & Conti, 2014; Kissling & Barrett, 2013; Kohn, Graham, Morton, Doyle, & Barrett, 1996; Ruiz-Martin et al., 2018) and within species (Ness et al., 2010; Shao et al., 2019; Zhou et al., 2017). However, none of these studies identified the molecular basis of such transitions, likely because the necessary genomic resources have only recently become available.

Recent studies in *Primula* revealed that the transition from heterostyly to homostyly is achieved *via* disruption of either *GLO?* or *CYP?*. Silencing *GLO?* caused a reduction of anther height in S-individuals, leading to the expression of short-homostyly in *Primula forbesii* (Huu, Keller, Conti, Kappel, & Lenhard, 2020). However, heteromorphic SI was retained, preventing self-fertilization and possibly explaining, together with the lower mutation rate of *GLO?* than *CYP?*, the low frequency of short-homostyles observed in nature (Huu et al., 2020). Similarly, a transposable element insertion likely compromising the function of *GLO?* was detected in one short-homostyle of a cultivated *P. vulgaris* variety (Li et al., 2016). Conversely, silencing *CYP?* in S-individuals of *P. veris* increased stigma height, causing the shift to long-homostyly (Huu et al., 2016). Correspondingly, the expression of *CYP?* was reduced in long-homostyles compared to S-individuals of both *P. vulgaris* and *P. oreodoxa* (Huu et al., 2016; Zhao, Luo, Yuan, Mei, & Zhang, 2019). Furthermore, all five exons of *CYP?* were likely lost in long-homostyles of the ancestrally heterostylous *P. forbesii*, whereas exon three of *CYP?* was not detected by PCR assays in the long-homostylous *P. grandis, P. halleri,* and *P. scotica* (Huu et al., 2016). Moreover, two loss-of-function mutations in *CYP?* were reported in self-compatible long-homostyles of *P. vulgaris,* suggesting that *CYP?* might additionally be involved in the control of SI (Li et al., 2016), but this has not been experimentally demonstrated (Kappel, Huu, & Lenhard, 2017). The findings above demonstrate that any genetic changes disrupting the function or expression of *CYP?*, a gene present only in S-individuals, cause long-homostyly. However, comprehensive analyses of the different types of mutations associated with shifts to homostyly based on extensive sampling of heterostyles and homostyles from multiple natural populations have never been performed.

After homostyles originate, their reproductive advantages over heterostyles should prompt changes in floral morph composition and genetic diversity of populations. Previous theoretical models predicted that homostyles should increase in frequency by replacing S-individuals (Crosby, 1949; 1960). Concomitantly, occasional crosses between homostyles and L-individuals and reduced fitness of homostyles, presumably caused by homozygosity of genes at the S-locus, were expected to prevent the fixation of homostyly (Crosby, 1949; 1960). Both mechanisms should ultimately result in the co-occurrence of homostyles with L-individuals, the latter remaining at low frequency. The predictions above were supported by two surveys of the frequency of L-, S- and homostylous individuals from natural populations of *P. vulgaris* performed at a 36-yr. interval (Crosby, 1949; Curtis & Curtis, 1985). Subsequent studies testing whether homostyles were affected by inbreeding depression found no evidence of seed-mass differences between heterostyles and homostyles

(Piper, Charlesworth, & Charlesworth, 1986). However, inbreeding depression at subsequent life-cycle stages has never been investigated. At the population genetic level, higher selfing in homostyles should increase homozygosity, thus decreasing diversity within and increasing differentiation among populations (Hamrick & Godt, 1996). These microevolutionary consequences of mating system transitions have been quantified only in a few homostylous species (Ness et al., 2010; Yuan et al., 2017; Zhou et al., 2017; Zhong et al., 2019).

Primula vulgaris Huds. (the common primrose) represents a classical model for the study of heterostyly and intraspecific transitions to homostyly (Bodmer, 1958; Cocker et al., 2018; Crosby, 1959; Piper et al., 1986). While distylous populations consisting exclusively of L- and S-individuals are common throughout Eurasia, mixed populations with varying frequencies of long-homostylous, S-, and L-individuals have been reported and widely documented for decades only in Somerset, England (Crosby, 1940; Curtis & Curtis, 1985). The occurrence of homostyles in multiple populations and the wide variation in their frequency in this region prompted Crosby (1949) to suggest that homostyles migrated from an initial center of origin to neighboring populations. However, two different loss-of-function mutations in *CYP?* were recently detected in two long-homostyles from different natural populations of *P. vulgaris* in England (Li et al., 2016), suggesting that homostyly might arise independently rather than *via* migration. Therefore, population genetic analyses aimed at clarifying the role of migration in the spread of homostyly are needed.

This study investigates the origins of homostyly, its effects on the mating system, and its population genetic consequences using the well-characterized *P. vulgaris* model. We thus combined surveys of floral morph frequencies from multiple natural populations of the ancestrally heterostylous *P. vulgaris* with both DNA sequence analyses of *CYP?* and microsatellite data from multiple individuals to ask the following questions: 1) Is an increase in the frequency of homostyles associated with a reduction of S-individuals and the maintenance of L-individuals at low frequencies, as predicted by Crosby's (1949) model and found in earlier studies (Curtis & Curtis, 1985)? 2) Is the transition to homostyly associated with a single or multiple molecular changes in *CYP?* and which ones? 3) Is the loss of heterostyly accompanied by a shift from outcrossing to selfing? And, if so, is there evidence of inbreeding depression as well as increased inbreeding within and genetic differentiation among populations? Our study generates new knowledge on the molecular basis of transitions from outcrossing to selfing, its evolutionary consequences, and the putative mechanisms precluding the fixation of homostyly within species.

2 METHODS

2.1 Study species

The ancestrally heterostylous *Primula vulgaris* is a perennial, rosette-forming diploid (2n = 22) blooming in early spring (February–April) with pale-yellow fused corollas reaching up to 40 mm in width formed by broad, overlapping, v-notched lobes (Richards, 2003). *Primula vulgaris* has dimorphic pollen grains and stigma papillae (Mast, Kelso, & Conti, 2006). Pollen grains are small in L-individuals but large in S-individuals, whereas stigma papillae are long in L-individuals but short in S-individuals (Richards, 2003). The species reproduces mainly sexually; clonal reproduction, uncommon in the wild, has been reported under cultivation (Boyd, Silvertown, & Tucker, 1990). Pollination in natural populations of *P. vulgaris* is mostly performed by long-tongued bees, bumblebees, and bee-flies, but butterflies, pollen-gathering bees and moths have been occasionally reported (Boyd et al., 1990; Keller et al., 2020; Woodell, 1960). Seeds, produced in capsules, are dispersed by ants and rodents (Valverde & Silvertown, 1995). *Primula vulgaris* has a patchy distribution with populations ranging from dozens to hundreds of individuals mostly found in woodlands and hedgerows and less frequently in grasslands (Jacquemyn, Endels, Brys, Hermy, & Woodell, 2009). Previous studies indicated that long-homostyles of *P. vulgaris* are self-compatible and produce seeds in the absence of pollinators (Piper et al., 1986). Analyses of the mating system of homostyles estimated a range of outcrossing rates from 0.05 to 0.8 (Bodmer, 1958; Crosby, 1959; Piper, Charlesworth, & Charlesworth, 1984). It has been suggested that reduced pollinator service due to intensive pastoral and agricultural activities could be the selective pressure favoring the increase of self-fertilizing homostyles in Somerset, England (Piper et al., 1986). Recently, long-homostyles have been reported in one population of an agriculturally fragmented area in the Netherlands (Barmentlo, Meirmans, Luijten, Triest, & Oostermeijer, 2017).

2.2 Frequency variation of floral morphs in natural populations of Primula vulgaris

To test whether homostyles increase concomitantly with the decrease of S-individuals, while L-individuals are maintained at low frequencies, we quantified floral morph composition in 22 natural populations of the Somerset region (England) in the spring of 2019 (Figure 2A). The approximate location of these populations was based on Curtis and Curtis (1985). The frequency of floral morphs was estimated by randomly scoring 100 individuals whenever possible (Table 1). Flowering plants were visually assigned to S-, L- and H-morphs (Figure 1). To determine whether S- and L-morphs segregated at equal frequencies in both dimorphic heterostylous (i.e., populations consisting of S- and L-individuals) and trimorphic populations (i.e., populations consisting of S-, L- and H-individuals), we tested whether morph ratios deviated significantly from isoplethy (i.e., equal frequencies of S- and L-morphs) using G-tests of goodness-of-fit as implemented in the R package 'DescTools' v0.99.38 (Signorell et al., 2020). We estimated a ternary plot using the R package 'ggtern' v3.1.0 (Hamilton & Ferry, 2018) to assess whether the increase in the frequency of H-morphs occurred at the cost of only one or both S- and L-morphs.

2.3 Sampling for genetic analyses

In the spring of 2019, we randomly collected leaf tissue from 11 to 30 individuals in each of the 22 natural populations described above for a total of 613 individuals. Leaf tissue was dried in silica gel. We sampled the same number of each floral morph where possible; sampled individuals were at least 1–2 meters apart from each other. We additionally collected leaf tissue and 2–3 capsules with seeds from nine individuals (four pins and five thrums) of one dimorphic heterostylous population (D07) and seven individuals from the fully homostylous population (M01). Collected seeds from each individual were sowed in a single pot; seedlings from a single individual formed a family. All pots were placed in water containing gibberellic acid (70 ppm) for 24 hours and later placed in growth chambers at 18 °C with a 12:12 h light-dark period. The proportion of germinated seeds per family was recorded after eight weeks, and leaf tissue from a total of ten seedlings per family was collected whenever possible and dried in silica gel. DNA of individuals from natural populations and progeny arrays was extracted with a modified CTAB protocol (Doyle & Doyle, 1987) and used for subsequent genetic analyses.

2.4 Molecular basis of the transition to homostyly

To determine whether the transition to homostyly is associated with a single or multiple molecular changes in *CYP?* and which ones, we sequenced *CYP?* from multiple S-individuals and homostyles of *P. vulgaris* from different populations.

Data generation - We Sanger-sequenced all five exons of *CYP?* from 38 individuals (27 H-individuals from 10 populations and 11 S-individuals from five populations, corresponding to 2–3 individuals per population). Additionally, we obtained *CYP?* sequences from whole genome resequencing data of six S-individuals from two populations (three individuals per population; EMC, unpublished data). Finally, we complemented our data set with previously published sequences from two H-individuals (*CYP?* S^{LH1} and S^{LH2}, respectively, of Li et al., 2016). In total, we thus analyzed *CYP?* sequences from 46 individuals (29 H- and 17 S-morphs).

For Sanger sequencing, we used previously designed primers based on all five *CYP?* exons (Huu et al., 2016). Reverse primers for exons 1, 2, and 3 were newly designed to obtain longer sequences (Supplementary material Table S1). Detailed PCR conditions for the amplification of all *CYP?* exons are included in Supplementary Material. Sanger sequencing was performed in an ABI Prism 3130 genetic analyzer (Applied Biosystems). Forward and reverse sequences were visually inspected and aligned with MUSCLE, as implemented in MEGA X (Kumar, Stecher, Li, Knyaz, & Tamura, 2018). All exon sequences were concatenated with Mesquite v3.61 (Maddison & Maddison, 2019). Library preparation and high throughput sequencing for the whole genome resequencing data were performed by RAPiD GENOMICS (Gainesville, Florida, USA) using paired-end sequencing (~150bp sequence reads) in NovaSeq 6000 (Illumina). We used HybPiper v1.3.1 (Johnson et al., 2016) with default parameters (except for the coverage-cutoff level for assemblies set to 4) to target and extract the sequence of *CYP?* from whole genome resequencing data. To identify synonymous and nonsynonymous mutations, we used the Open Reading Frame (ORF) from *P. vulgaris CYP?* sequence

deposited in GenBank (KT257665.1; Li et al., 2016).

Analyses – To determine the extent of *CYP?* variation in S-individuals and homostyles, we estimated nucleotide diversity at synonymous (πS) and nonsynonymous sites (πNS) using DNAsp v6.12.03 (Rozas et al., 2017). To determine the relationships among *CYP?* sequences from H- and S-individuals, we first estimated a haplotype network with the R package 'pegas' v0.12 (Paradis, 2010). Such analysis is appropriate because *CYP?* is located in the hemizygous, non-recombining S-locus. In addition to single nucleotide substitutions, we scored each insertion or deletion (i.e., indel) as a character following the "simple indel contig" guidelines by Simmons and Ochoterena (2000). Briefly, each indel of any length was scored as a presence/absence character in every individual. The resulting presence/absence matrix was coded as pseudo-nucleotides using 'A' as absence, 'T' as presence and '-' as unknown, and was concatenated to the sequence alignment of *CYP?*. Secondly, we estimated the *CYP?* phylogeny using a partitioned Maximum Likelihood (ML) analysis in RAxML v8.01 (Kozlov, Darriba, Flouri, Morel, & Stamatakis, 2019) with a GTR-GAMMA substitution model for nucleotide substitutions and a binary (BIN) model for indels. Branch support was estimated with 1000 standard bootstrap re-samplings. A publicly available *CYP?* sequence from *P. veris* (KX589238; Huu et al., 2016) was used as an outgroup to root the *CYP?* tree.

2.5 Evolutionary consequences of transitions to homostyly

We tested whether outcrossing rates from progeny arrays are higher in heterostyles than homostyles with microsatellites. We estimated the strength of inbreeding depression at the seed-germination stage. We tested whether increasing frequencies of homostyles are associated with higher population-level selfing rates, inbreeding coefficients within populations, and genetic differentiation among populations.

2.5.1 Outcrossing rates from progeny arrays

Outcrossing rates were estimated from nine heterostylous families (stemming from the dimorphic heterostylous population D07) with a mean number of 10 seedlings per family and seven homostylous families (stemming from the fully homostylous population M01) with 7.86 ± 1.06 (mean ± SE) seedlings per family. Both maternal and seedling plants were genotyped with the same microsatellites as in section 2.5.2. Multi-locus (t_m) and single-locus (t_s) outcrossing rates and their associated standard errors were estimated with MLTR v.3.4 (Ritland, 2002), using 10000 bootstrap resamplings of maternal families. We used a one-sided Wilcoxon signed-rank test to assess whether homostylous individuals have a lower outcrossing rate than distylous individuals. Moreover, the germination rate of heterostylous and homostylous families was used as a fitness proxy to estimate the strength of inbreeding depression (δ) as $1 - (W_{HO} \,/\, W_{HE})$ (Goodwillie, Kalisz, & Eckert, 2005) where W_{HO} and W_{HE} are the mean germination rates of homostyles and heterostyles, respectively.

2.5.2 Population-level estimates of selfing rates

Data generation - We genotyped all 613 individuals collected from the 22 natural populations using 12 microsatellites previously developed for *P. vulgaris* (Triest, Sierens, & Van Rossum, 2015). Briefly, the loci were amplified in two multiplex reactions with a QIAGEN Multiplex PCR kit. Detailed conditions for the amplification of microsatellites are included in Supplementary Material. Fragment size estimations were performed using an ABI Prism 3130xl genetic analyzer (Applied Biosystems) with GeneScan 500 LIZ (Applied Biosystems) as internal standard. Alleles were scored using GeneMapper v4.1 (Applied Biosystems). The presence of null alleles was estimated with Micro-checker v2.2.3 (Van Oosterhout, Hutchinson, Wills, & Shipley, 2004).

Analyses – Population-level selfing rates were inferred using model-based Bayesian estimation (BES v0.1.3; Redelings et al., 2015) from microsatellite data of 613 individuals from 22 natural populations (see section 2.3). The main advantage of this method compared to estimates generated by other programs such as RMES (David, Pujol, Viard, & Goudet, 2007) is that BES makes use of all loci regardless of whether they are homozygous or heterozygous. Selfing rates and 95% CIs were inferred using 10000 bootstrap iterations. To test whether higher frequencies of homostyles in natural populations are associated with higher selfing rates, we used generalized additive models where the frequency of homostyles was used as an independent

variable and by specifying a beta distribution for the estimates of selfing rates as implemented in the R package 'gamlss' v5.1.6 (Rigby, Stasinopoulos, & Lane, 2005).

2.5.3 Population genetic analyses

Allelic richness (Ar), observed (H_o) and expected heterozygosity (H_e), and inbreeding coefficient (F_{is}) were calculated with the R package 'diveRsity' v9.90 (Keenan, Mcginnity, Cross, Crozier, & Prodöhl, 2013) from microsatellite data of 613 individuals from 22 populations (see section 2.3). Each locus and population were tested for Hardy-Weinberg equilibrium using the R package 'genepop' v1.1.7 (Rousset, 2008). To assess whether an increase in the frequency of homostyly is associated with an increase in F_{is}, we used a standard linear model with homostyle frequency as the independent variable. Given that population size can influence F_{is}, we included census size as covariable with no interaction among independent variables.

Pairwise genetic differentiation measured as F_{st} (Weir & Cockerham, 1984) and its normalized counterpart G'_{st} (Meirmans & Hedrick, 2011) were estimated with the R package 'diveRsity' v9.90 (Keenan et al., 2013). To discover whether higher homostyle frequencies increase genetic differentiation, we tested whether pairwise differences in homostyle frequencies between populations are positively correlated with pairwise G'_{st} values. To test the significance of association between these two matrices, we used a Mantel test as implemented in the R package 'adegenet' v2.1.3 (Jombart, 2008).

2.6 Genetic structure and gene flow

To estimate genetic structure among *P. vulgaris* populations, we used InStruct v3.2.09 (Gao, Williamson, & Bustamante, 2007), which extends the Bayesian model implemented in Structure (Pritchard, Stephens, & Donnelly, 2000) to situations of partial self-fertilization and recurrent inbreeding. We ran the analyses with 100000 burn-in iterations and 20 independent MCMC chains per run from 2 to 22 k, as suggested by Gilbert et al. (2012). The most likely number of clusters (k) was detected with the $\Delta\kappa$ method (Evanno, Regnaut, & Goudet, 2005) implemented in CLUMPAK (Kopelman, Mayzel, Jakobsson, Rosenberg, & Mayrose, 2015). Additionally, a Discriminant Analysis of Principal Components (DAPC) was performed with the R package 'adegenet' v2.1.1 (Jombart, 2008). To determine whether there is Isolation By Distance (IBD), we performed a Mantel test implemented in 'adegenet' using both F_{st} and G'_{st} values of genetic differentiation.

Finally, to determine whether patterns of genetic structure are explained by gene flow, we estimated the size-corrected effective number of migrants per generation (Nm) using the frequency of private alleles with the R package 'genepop' v1.1.7 (Rousset, 2008). Moreover, we used Approximate Bayesian Computations (ABC), as implemented in popABC v1.0 (Lopes, Balding, & Beaumont, 2009), to compare models of genetic divergence with and without gene flow using the coalescent framework developed by Nielsen and Wakely (2001) and Hey and Nielsen (2004). Specifically, we compared a scenario of isolation without gene flow (i.e., proportion of migrants per generation, $m = 0$) with seven scenarios of increasing migration rates ($m = 0.001$, 0.01, 0.1, 0.2, 0.3, 0.4 and 0.5). Priors used for this analysis are specified in Supplementary Material (Table S2). Each model was simulated with 100000 iterations and tolerance for the rejection step was set to 0.01. Model selection was based on the posterior probability estimated by categorical regression (Beaumont, Zhang, & Balding, 2002) using custom R scripts included in the popABC documentation. A major assumption of the models implemented in popABC is that there is no genetic structure within populations. Given that H-individuals may cause within-population structure due to selfing, we decided to use only the ten dimorphic heterostylous populations for popABC analyses because no genetic substructure is expected in populations consisting entirely of outcrossing individuals. No differences in pollen and seed dispersal are known for H-, S- and L-individuals, thus excluding populations with H-individuals from popABC analyses should not affect estimates of migration between populations.

3 RESULTS

3.1 Frequency variation of floral morphs in natural populations of Primula vulgaris

The frequency of homostyles ranged from 0% to 100% across the 22 sampled populations of *P. vulgaris* in Somerset, England (Table 1; Figure 2A). Ten populations were dimorphic heterostylous (L- and S-

individuals; D01–D10), one was dimorphic with L- and H-individuals (D*11), ten were trimorphic (L-, S- and H-individuals; T01–T10), and one was monomorphic for the H-morph (M01). Morph ratios in dimorphic heterostylous populations did not deviate from isoplethy except in D02 and D08, which had an excess of L- and S-plants, respectively ($G = 7.13$, $P = 0.007$ and $G = 6.11$, $P = 0.01$, respectively; Supplementary material Table S3). In trimorphic populations, L-individuals were significantly more frequent than S-individuals except in T03, where S- and L-morph frequencies did not differ significantly ($G = 0.13$, $P = 0.71$; Supplementary material Table S3). Congruently, the ternary plot suggested a skewed trajectory towards a reduction of S-individuals when H-individuals were present (Figure 2B).

3.2 Molecular basis of the transition to homostyly

We sequenced ˜97% of the 1,587 bp comprising the five exons of *CYP?* from 17 S- and 27 H-individuals of *P. vulgaris* from seven and ten populations, respectively. In total, we detected seven *CYP?* alleles (*CYP?-1* to *-7*; Figure 3A). All 17 S-individuals shared the same allele (*CYP?-1*), identical to the functional copy of *CYP?* previously reported in *P. vulgaris* (GenBank: KT257665.1; Li et al., 2016). Unexpectedly, the putatively functional *CYP?-1* allele also occurred in six H-individuals. In the 21 remaining H-individuals, we detected six *CYP?* alleles (*CYP?-2* to *-7*), comprising altogether a single synonymous mutation, four nonsynonymous mutations, and two deletions. Specifically, *CYP?-4* contained two private mutations (one synonymous and one nonsynonymous) and five *CYP?* alleles contained a single private mutation (three different nonsynonymous mutations in *CYP?-2, -3, -7* and two different deletions in *CYP?-5* and *-6*). The nonsynonymous mutation in *CYP?-2* introduced a premature stop codon in exon 2, whereas a 31 bp deletion in exon 5 of *CYP?-5* and an 8 bp deletion in exon 1 of *CYP?-6* introduced a frameshift leading to an early stop codon. Moreover, a mutation in exon 5 of *CYP?-3* changed a non-polar (phenylalanine) to a polar amino acid (serine), whereas a mutation in exon 3 of *CYP?-4* changed an amidic (asparagine) to a hydroxylic (serine) amino acid. Finally, the arginine to histidine mutation in *CYP?-7* caused no change in amino acid side-chain polarity. Overall, nucleotide diversity in homostyles was $\pi S = 0.0005$ and $\pi NS = 0.001$, while S-morph individuals showed no genetic variation in *CYP?* (both πS and πNS were zero).

In the haplotype network, *CYP?-1*, the known functional allele, occupied a central node and was connected by a single mutational step to all other alleles except for *CYP?-5,* which differed by two mutational steps (Figure 3B). Additionally, our phylogenetic analysis recovered lack of structure in the backbone of the inferred tree but well-supported clades where individuals sharing the same *CYP?* allele are grouped together (Figure 4). Specifically, *CYP?-2* was shared among homostyles from different populations (T03, T04, T07, T10, and D*11; Figure 4); *CYP?-3* was unique to population T05, and *CYP?-5* was unique to population T09. Finally, two *CYP?* alleles were detected in each of three populations: *CYP?-4* and *CYP?-6* were found in population T06, *CYP?-2* and *CYP?-4* in population T10, and *CYP?-2* and *CYP?-7* in population D*11 (Figure 4).

3.3 Evolutionary consequences of transitions to homostyly

Mating system in homostyles - Outcrossing rates estimated from progeny arrays were more variable and significantly lower in homostylous than heterostylous families (single locus [t_s]: mean ± SE; 0.24 ± 0.10 [homostylous] and 0.83 ± 0.05 [heterostylous]; multi-locus [t_m]: 0.14 ± 0.06 and 0.98 ± 0.02, respectively; Wilcoxon signed-rank test $W = 63$, $P = 0.002$ and 0.001; Figure S1). As expected, the frequency of homostyles within populations was positively associated with population-level estimates of selfing rate (*pseudo-*R^2 = 0.447, $P < 0.001$; Table 1, Figures 5A). Seed germination rate was significantly lower for homostyles than heterostyles (0.11 ± 0.03 vs. 0.26 ± 0.05; $W = 308$, $P = 0.04$) resulting in an estimated inbreeding depression (δ) of 0.58.

Patterns of genetic diversity – Eighteen out of 22 populations (except for D03, D06, D08 and D10) had significant deviations from Hardy-Weinberg equilibrium due to a heterozygote deficit (Supplementary Table S4). Population-level estimates of allelic richness (Ar) varied from 1.58 to 3.78 (mean ± SE, 3.19 ± 0.09), expected heterozygosity (H_e) from 0.14 to 0.53 (0.42 ± 0.01), and observed heterozygosity (H_o) from 0.11 to 0.46 (0.37 ± 0.02). Inbreeding coefficient (F_{is}) ranged from -0.08 to 0.39 among populations (0.13 ±

0.02; Table 1) and had a significant positive relationship with the frequency of homostyly ($R^2 = 0.405$, $P = 0.03$), but not with population size ($P = 0.27$; Figure 5B).

Global values of genetic differentiation among populations were 0.083 (95% CI: 0.074–0.093) and 0.164 (95% CI: 0.147–0.181) for F_{st} and G'_{st}, respectively (Table S4), and were strongly correlated with each other (*pseudo*-$R^2 = 0.974$, $P = 0.001$). Pairwise population values of F_{st} and G'_{st} are shown in Supplementary Material Table S5. As expected, pairwise homostyle frequencies showed a significant positive relationship with pairwise G'_{st} (Mantel test: $R^2 = 0.481$, $P < 0.001$).

3.4 Genetic structure and gene flow

InStruct analyses recovered two clusters (Figure 6A) and showed that T08 differs from the remaining 21 populations. Identical results were found with Structure (results not shown). Accordingly, the DAPC analyses separated T08 from the rest of the populations (Figure 6B). Furthermore, we found no evidence of isolation by distance (Mantel test, $P = 0.457$). Together, these results suggest that genetic differentiation among populations is moderate, corroborating F_{st} results presented above. Using the frequency of private alleles, we estimated that the effective number of migrants per generation (Nm) was 1.96. Comparison of different demographic scenarios lent higher support to models with inter-population gene flow than to the isolation model. Among the models with varying migration rates (m), the one with $m = 0.2$ had the highest posterior probability, indicating moderate gene flow (Figure S2).

4 DISCUSSION

The present study of shifts from heterostyly to homostyly provides novel insights into the molecular basis of intraspecific mating system transitions and their evolutionary consequences. Previous studies suggesting independent origins of homostyly used molecular markers not associated with the genetic control of heterostyly (Ness et al., 2010; Shao et al., 2019; Yuan et al., 2017; Zhou et al., 2017). By leveraging new knowledge on the molecular basis of heterostyly and extensive sampling of populations with different frequencies of homostyles, this is the first study to demonstrate that heterostyly has been repeatedly lost likely *via* multiple, presumably loss-of-function mutations of the S-locus gene controlling stigma position (*CYP?*). Additionally, we show that the transition to homostyly promotes a change of mating system from outcrossing to selfing, with ensuing population genetic consequences. Furthermore, we discuss the potential roles of gene flow in the spreading of homostyly. Finally, we propose that inbreeding depression might explain why homostyly, despite its apparent advantages, has not become fixed in *P. vulgaris*. Thus, the present contribution provides a benchmark for similar studies on the loss of heterostyly across angiosperms.

4.1 Homostyles replace short-styled individuals within populations

The variation in the frequency of floral morphs among populations provides an opportunity to elucidate how homostylous phenotypes originate and spread. According to previous evolutionary models, the origin of homostyles from S-individuals should cause an initial reduction of the latter, triggering an increase in the number of homostyles (Crosby, 1949; 1959). When homostyles first arise, their pollen can be used for both self- and cross-fertilization of L-individuals, but not for fertilization of S-individuals, due to lack of spatial reciprocity between high anthers of homostyles and low stigma of S-individuals and incompatibility between homostyle pollen and S-morph stigmas (Crosby, 1949; Figure 1). Furthermore, homostyles can be fertilized by compatible pollen of S-morphs, but this cross is thought to occur rarely in nature due to stigma clogging with self-pollen in homostyles (Crosby, 1959; but see Bodmer, 1959). Hence, homostyles have a reproductive advantage over L- and S-morphs stemming from their ability to fertilize both themselves and the L-morphs (Richards, 2003). Finally, self-fertilization of homostyles (Figures S3A and B) and occasional crosses from homostyles to L-individuals produce homostylous and L-progeny, but no S-progeny (Figures S3C and D).

Congruently with Crosby's predictions (1949) and findings from previous studies (Curtis & Curtis, 1985), our results demonstrate that, as homostyles increase, more S- than L-individuals are lost within populations (Table 1 and Figures 2A and B). After 72 and 36 years since Crosby's (1949) and Curtis and Curtis (1985) observations, respectively, we also found that homostyly has not become fixed in Somerset populations. Fur-

thermore, the fact that L-individuals are maintained at low frequencies, even in the absence of S-individuals, suggests that they are occasionally fertilized by homostyles. Experiments aimed at quantifying pollen delivery and receipt among the three floral morphs would help to clarify the selective regimes favoring the increase of homostyles. Overall, our results are consistent with the hypothesis that long-homostyles originate from S-individuals and explain why the latter occur at lower frequencies than L-individuals across populations with all three morphs.

4.2 Multiple losses of heterostyly within species are associated with different molecular changes in the CYP? gene

Recent advancements in genomics have enabled the identification of loci responsible for repeated losses of phenotypic traits (Albalat & Cañestro, 2016; Sharma et al., 2018). For instance, multiple loss-of-function mutations were detected in *SCR* or *SCR*-like genes corresponding to independent losses of self-incompatibility in *Arabidopsis thaliana* and *Laevenworthia alabamica* (Chantha et al., 2013; Shimizu et al., 2008). In the case of homostyly, recent experimental studies established that *CYP?* disruption causes a shift to homostyly (Huu et al., 2016; Kappel et al., 2017). Accordingly, all S-individuals of *P. vulgaris* analyzed in the present study share the same functional *CYP?* allele (*CYP?-1*), whereas private alleles with nonsynonymous mutations or indels (*CYP?-2* to *-9*) are found exclusively in homostyles (Figures 3A, 3B and 4). These mutations cause either changes in the polarity of the amino acid side chain (*CYP?-3* and *-4*) or premature stop codons (*CYP?-2*, *-5* and *-6*), both types of mutation presumably inducing loss or reduction of function (Zhang, 2000). In one case (*CYP?-7*), a nonsynonymous mutation did not change amino acid side-chain polarity; thus, this mutation may or may not affect protein function (Figure 3A). Notably, the alleles found in our study differ from the ones previously reported in two long-homostyles of *P. vulgaris* (*CYP?-8* and *-9*, originally named *CYP? S^{LH1}* and S^{LH2}, respectively; Li et al., 2016). Thus, a total of eight different putative loss-of-function mutations in *CYP?* have been identified so far in homostylous individuals of *P. vulgaris*. Future work should focus on elucidating how the found nonsynonymous mutations affect *CYP?* function. Finally, the groupings of the haplotype network were congruent with those of the phylogeny (Figures 3B and 4), as expected given the lack of recombination in the S-locus, hence *CYP?*. Overall, our results show that a diversity of changes in the same gene is associated with multiple, independent origins of homostyly within species.

Loss of phenotypic traits can be caused by mutations not only in coding regions of specific genes but also in their promoter regions or by structural rearrangements. For instance, some individuals of self-compatible *A. thaliana* were characterized by mutations in *cis*-regulatory regions, inversions, or splicing variants, causing loss of function in *SCR* or *SRK* genes controlling self-incompatibility (Dwyer et al., 2013; Shimizu et al., 2008; Shimizu & Tsuchimatsu, 2015). In *P. vulgaris*, a surprising result is that six out of 27 homostyles have the same *CYP?* allele as the S-individuals (*CYP?*-1; Figures 3A, 3B and 4). These six homostyles occur in two geographically close populations (M01 and T08; Figures 2A). The occurrence of a *CYP?* allele with no mutations in homostyles enables us to suggest for the first time that additional mechanisms might be responsible for the inactivation of *CYP?*, including mutations in its promoter region or structural rearrangements that cannot be detected *via* exon sequencing. In general, this result underscores that mutations outside genes controlling specific traits might represent essential sources for repeated trait losses.

The interpretation of *CYP?* sequencing results presented above is compatible with multiple origins of homostyly in *P. vulgaris*, but alternative scenarios involving a single origin should be considered. For example, as discussed above, the initial homostylous phenotype could have arisen *via* mutations in the promoter region, structural rearrangements, or changes in the expression of *CYP?* but not in the *CYP?* coding region *per se*, as in the six homostyles carrying *CYP?-1,* the haplotype of S-morphs. Such homostyle could have originated once in a large ancestral population that later became fragmented and/or migrated to neighboring populations, gaining nonsynonymous mutations and indels in *CYP?* after the gene had already been rendered functionless. However, in the scenario of a single origin of homostyly triggered by a mutation outside CYP^{T}, we would expect homostyles carrying *CYP?-1* to co-occur in the same population with other homostyles carrying mutated *CYP?* alleles (i.e., *CYP?-2 to -9*), but our findings do not match this prediction (Figure 4). Thus, the most parsimonious interpretation of the haplotype network and phylogeny inferred from *CYP?*

sequences (Figures 3 and 4) is congruent with multiple origins of homostyly *via* independent mutations at *CYP?*. Furthermore, *CYP?-9* (S^{LH2} from Li et al., 2016) was found exclusively in a homostyle from Chiltern Hills located approximately 200 km from Somerset. Given the limited dispersal abilities reported for *P. vulgaris* (Cahalan & Gliddon, 1985), this finding further supports independent origins of homostyly. Future transcriptomic or RT-PCR analyses of homostyles with different *CYP*? alleles aimed at testing the expression of both mutated and unmutated *CYP*? should further elucidate the question of single vs. multiple origins of homostyly in *P. vulgaris*. Finally, our microsatellite data do not enable us to determine whether mutations in *CYP*? accumulated before or after the fragmentation of a hypothetical ancestral population. Whole genome sequences from multiple heterostyles and homostyles aimed at improving phylogenetic resolution and demographic analyses are necessary to elucidate the potential role of fragmentation in the evolution of *P. vulgaris* homostyles.

The multiple *CYP?* mutations found in the homostyles of a small geographic region in Somerset could be viewed as a puzzling result. However, loss of gene function is usually followed by degeneration through accumulation of mutations, or even gene loss (Sharma et al., 2018). Additionally, lack of recombination and hemizygosity of the S-locus should both decrease the efficacy of purifying selection on its genes, including *CYP?,* possibly contributing to accumulation of mutations (Becher, Jackson, & Charlesworth, 2020; Gossmann, Woolfit, & Eyre-Walker, 2011). Furthermore, a higher mutation rate was reported for *CYP?* than *GLO?* (Huu et al., 2020). Thus, the multiple *CYP?* mutations of homostyles detected here are compatible with both theoretical expectations and previous empirical evidence. Future sequences of other S-locus genes, their paralogs, and additional genes outside the S-locus from both *P. vulgaris* and other primroses would provide a broader context to compare selection on *CYP?* vs. other genes in both homostyles and heterostyles.

4.3 Consequences of shifts to homostyly on mating system and population genetics

Changes in floral morphology can have profound effects on the mating system (Opedal, 2018). Specifically, the reduction of anther and stigma separation and loss of self-incompatibility of homostylous morphs should increase selfing compared to heterostyles. Evidence of this mating system transition in homostyles was reported for *Eichhornia* (Husband & Barrett, 1993), *Turnera* (Belaoussoff & Shore, 1995), *Amsinckia* (Schoen et al., 1997), and some *Primula* species (Yuan et al., 2017; Zhou et al., 2017; Zhong et al., 2019). In *P. vulgaris*, previous estimates of outcrossing rates in homostyles ranged broadly from 0.05 to 0.80 (Bodmer, 1958, 1984; Crosby, 1958, Piper et al., 1986).

Our results from progeny arrays indicate that outcrossing rates in homostyles are significantly lower than in heterostyles (t_m = 0.14 vs. 1.0, respectively), as expected. Such outcrossing rates were estimated based exclusively on germinated seeds. However, ungerminated seeds were likely those with higher homozygosity, hence higher inbreeding depression, thus their inclusion would have further decreased our estimates of outcrossing rates. Also as expected, the frequency of homostyles was associated with an increase in population-level selfing rates (Figure 5A). Nevertheless, the fully homostylous population (M01) had lower selfing rates than expected, possibly caused by increased error rates due to its small sample size (Redelings et al., 2015). The estimated outcrossing rates of homostyles firmly place them in the category of selfers (i.e., t_m [?] 0.2; *sensu* Goodwillie et al., 2005; Schemske & Lande, 1985). Overall, our findings clarify previous conflicting results about the effects of homostyly on the mating system of *P. vulgaris*, confirming that transitions to homostyly increase selfing.

Mating systems shape how genetic diversity is partitioned within and among populations (Barrett, 2010; Wright et al., 2013). In concordance with theoretical expectations, we found that intrapopulation homostyle frequency significantly increased inbreeding coefficients (Figure 5B). These results conform with the reduction of genetic diversity associated with transitions from heterostyly to homostyly documented in other systems (Husband & Barrett, 1993; Ness et al., 2010; Yuan et al., 2017; Zhong et al., 2019; Zhou et al., 2017). Moreover, our population genetic results indicate that increased frequency of homostyles in populations increases homozygosity, thus lowering intrapopulation genetic diversity and elevating inter-population genetic differentiation. Altogether, our findings confirm the population genetic consequences predicted for

the transition to selfing.

4.4 Does homostyly spread among populations and why has it not become fixed in *Primula vulgaris?*

Gene flow plays a central role in spreading advantageous mutations (Morjan & Rieseberg, 2004; Ralph & Coop, 2010) and could favor the migration of homostylous alleles among populations. In *P. vulgaris,* it has been proposed that homostyles could have migrated from initial places of origin to neighboring populations through pollen or seed, the former being more likely (Crosby, 1949; 1960). Previous studies estimated that dispersal is restricted to a maximum of a few hundred meters from the parental plant in *P. vulgaris* (Cahalan & Gliddon, 1985). However, occasional pollen flow over 1–3 kilometers has been reported (Van Geert, Van Rossum, & Triest, 2010). Indeed, our population genetic results support a model of moderate gene flow among populations ($Nm = 1.96$; Figure S2) consistent with moderate genetic differentiation among populations ($F_{st} = 0.083$; Figures 6A and B), the latter being lower than previous estimates for *P. vulgaris* ($F_{st} = 0.086$–0.508; van Geert et al., 2015). Furthermore, we did not detect isolation by distance (Mantel test, $P = 0.457$), further favoring the hypothesis of gene flow. Moreover, the geographic distribution of *CYP?* alleles in our study indicates that 12 homostylous individuals from five populations (D*11, T03, T04, T07 and T10) separated by 3-18 Km shared the same *CYP?* allele (*CYP?*-2; Figure 4), suggesting that some homostyles could have migrated between neighboring populations. To summarize, Crosby (1949; 1959) proposed a single origin of homostyles followed by their spreading *via* migration. While supporting multiple origins of homostyly, our results imply that it can also spread *via* gene flow, providing partial corroboration of Crosby's hypothesis.

A crucial question remains as to why homostyly has not become fixed in *P. vulgaris* despite automatic selfing advantage (Fisher, 1941; 1949) and reproductive assurance (Piper et al., 1986). In fact, the opposite has been found, since previous studies recorded the loss or decrease of homostyles in revisited populations (Boyd et al., 1990; Curtis & Curtis, 1985). Crosby (1949) proposed that selfed progeny from homostyles homozygous for the S-locus should have reduced fitness, likely caused by potentially deleterious effects of dominant homozygosity in S-locus genes. Such negative effects were suggested by crossing experiments with S-morphs of *Primula sinensis* (Mather & de Winton, 1941) and *P. oreodoxa* (Yuan et al., 2018). However, whether homostyles with one or two copies of the S-locus have differences in fitness has not been experimentally tested.

An additional explanation for the failure of homostyly to completely replace heterostyly is that the negative effects of inbreeding depression (Goodwillie et al., 2005; Richards 1984) can outweigh the advantages of homostyly (Boyd et al., 1990; Piper et al., 1984). Theoretical models suggest that inbreeding depression values above 0.5 should prevent the invasion of selfing individuals in an outcrossing population (Lande & Schemske, 1985). Two recent studies investigated the relationship between inbreeding depression and the spread of self-compatibility, finding contrasting results. In experimental populations of *Linaria cavanillesi*, self-compatible individuals with no inbreeding depression displaced self-incompatible individuals in just three generations (Voillemot & Pannell, 2017; Voillemot, Encinas-Viso, & Pannell, 2019). In contrast, inbreeding depression values of 0.54 prevented the spread of self-compatible plants in experimental patches of self-incompatible plants in *Laevenworthia alabamica* (Layman, Fernando, Herlihy, & Busch, 2017). Our estimate of inbreeding depression at seed germination stage (0.58) in *P. vulgaris* is closer to the latter study and above the threshold value of 0.5 predicted to prevent the invasion of selfing (Lande & Schemske, 1985). The effect of inbreeding depression in *P. vulgaris* might be even higher than in our current estimates, for it could also act at later stages of the life cycle. Altogether, our results imply that inbreeding depression in homostyles is sufficiently high to prevent the fixation of homostyly within populations.

While theory proposes that increased selfing should purge inbreeding depression over time by eliminating recessive deleterious alleles from populations (Schemske & Lande, 1985), transitions to homostyly in *P. vulgaris* may be too recent for the purging process to have occurred. Moreover, recessive deleterious alleles could have been re-introduced into populations *via* gene flow, thus slowing the decrease of inbreeding depression. Our study estimated moderate levels of gene flow among populations of *P. vulgaris* ($Nm = 1.96$; Supplementary

Figure S2), implying that re-introduction of genetic load can occur. In conclusion, our findings suggest that inbreeding depression contributes to maintaining heterostylous morphs within populations despite the reproductive advantages of homostyly.

ACKNOWLEDGMENTS

We thank Natural England for permits and landowners for access to populations; Lindsey and Derek Cullen for accommodation and assistance during fieldwork; Markus Meierhofer and Rayko Jonas for help in the greenhouse; Francesco Rivetti for assistance in the laboratory; Members of the Conti group for fruitful discussions. We thank Kathryn Hodgins and three anonymous reviewers for their comments that greatly improved this manuscript.

AUTHOR CONTRIBUTIONS

EMC, BK, JdV, PS and EC designed the research. EMC collected the data. EMC, RS and BK performed laboratory work. EMC, RS, EL-B and BK analyzed the data. EMC and EC wrote the paper and all authors provided feedback on the manuscript.

FUNDING

This research was supported by the Graduate Campus office at the University of Zurich through a GRC-Travel Grant to EMC, by the Swiss Government Excellence Scholarship grant no. 2018.0475 to EMC, and by the Swiss National Science Foundation grant nos. 3100-061674.00/1 and 31003A_175556 to EC. JdV is supported in part by Swiss National Science Foundation grant 310030_185251.

CONFLICT OF INTEREST STATEMENT

The authors declare that the research was conducted in the absence of any commercial or financial relationships that could be construed as a potential conflict of interest.

DATA AVAILABILITY STATEMENT

-Microsatellite genotypes from the 613 individuals from the 22 natural populations analyzed in this study, as well as DNA alignment for CYP^T haplotype network and phylogeny will be made available in Dryad.

-Scripts for analyses and figures in R are being curated and will be made available in Github.

REFERENCES

Albalat, R. & Cañestro, C. (2016). Evolution by gene loss. *Nature Reviews Genetics* 17, 379–391

Barmentlo, S. H., Meirmans, P. G., Luijten, S. H., Triest, L. & Oostermeijer, J. G. B. (2017). Outbreeding depression and breeding system evolution in small, remnant populations of Primula vulgaris: consequences for genetic rescue. *Conservation Genetics* **19**, 545–554.

Barrett, S. C. H. (1992). *Evolution and function of heterostyly.* Berlin, Germany: Springer-Verlag.

Barrett, S. C. H. (2010). Understanding plant reproductive diversity. *Philosophical Transactions of the Royal Society B: Biological Sciences, 365*(1537), 99–109. doi:10.1098/rstb.2009.0199

Barrett, S. C. H. (2019). 'A most complex marriage arrangement': Recent advances on heterostyly and unresolved questions. *New Phytologist, 224*(3), 1051–1067. doi:10.1111/nph.16026

Barrett, S. C. H., Ness, R. W., & Vallejo-Marín, M. (2009). Evolutionary pathways to self-fertilization in a tristylous plant species. *New Phytologist, 183*(3), 546–556. doi:10.1111/j.1469-8137.2009.02937.x

Beaumont, M. A., Zhang, W., & Balding, D. J. (2002). Approximate Bayesian Computation in population genetics. *Genetics, 162*(162), 2025–2035. doi:10.1111/j.1937-2817.2010.tb01236.x

Becher, H., Jackson, B. C. & Charlesworth, B. (2020). Patterns of genetic variability in genomic regions with low rates of recombination. *Curr. Biol.* 30, 94-100.e3

Belaoussoff, S., & Shore, J. S. (1995). Floral correlates and fitness consequences of mating-system variation in *Turnera ulmifolia*. *Evolution, 49*(3), 545–556. doi:10.2307/2410278

Bodmer, W. F. (1958). Natural crossing between homostyle plants of *Primula vulgaris*. *Heredity, 12*(3), 363–370.

Bodmer, W. F. (1960). The genetics of homostyly in populations of *Primula vulgaris*. *Philosophical Transactions of the Royal Society B: Biological Sciences, 242*(696), 517–549.

Bodmer, W. F. (1984). Sex and generations of primroses. *Nature, 310*, 731. doi:10.1038/310731a0

Boyd, M., Silvertown, J., & Tucker, C. (1990). Population ecology of heterostyle and homostyle *Primula vulgaris*: Growth, survival and reproduction in field populations. *Journal of Ecology, 78*(3), 799–813. doi:10.2307/2260900

Busch, J. W., & Delph, L. F. (2012). The relative importance of reproductive assurance and automatic selection as hypotheses for the evolution of self-fertilization. *Annals of Botany, 109*(3), 553–562. doi:10.1093/aob/mcr219

Cahalan, C. M., & Gliddon, C. (1985). Genetic neighbourhood sizes in *Primula vulgaris*. *Heredity, 54*, 65–70. doi:10.1038/hdy.1985.9

Carlson, M. L., Gisler, S. D., & Kelso, S. (2008). The role of reproductive assurance in the arctic: A comparative study of a homostylous and distylous species pair. *Arctic, Antarctic, and Alpine Research. 40*(1), 39–47. doi:10.1657/1523-0430(06-080)[CARLSON]2.0.CO;2

Chantha, S. C., Herman, A. C., Platts, A. E., Vekemans, X., & Schoen, D. J. (2013). Secondary evolution of a self-incompatibility locus in the Brassicaceae genus *Leavenworthia*. *PLoS Biology. 11*(5), e1001560. doi:10.1371/journal.pbio.1001560

Charlesworth, B., & Charlesworth, D. (1979). The maintenance and breakdown of distyly. *American Naturalist, 114*(4), 499–513. doi:10.1086/283497

Cocker, J. M., Webster, M. A., Li, J., Wright, J., Kaithakottil, G., Swarbreck, D., & Gilmartin, P. M. (2015). Oakleaf: An S locus-linked mutation of *Primula vulgaris* that affects leaf and flower development. *New Phytologist, 208*(1), 149–161. doi:10.1111/nph.13370

Cocker, J. M., Wright, J., Li, J., Swarbreck, D., Dyer, S., Caccamo, M., & Gilmartin, P. M. (2018). *Primula vulgaris* (primrose) genome assembly, annotation and gene expression, with comparative genomics on the heterostyly supergene. *Scientific Reports, 8*(1), 17942. doi:10.1038/s41598-018-36304-4

Costa, J., Torices, R., & Barrett, S. C. H. (2019). Evolutionary history of the buildup and breakdown of the heterostylous syndrome in Plumbaginaceae. *New Phytologist*, *224*(3), 1278-1289. doi:10.1111/nph.15768

Crosby, J. L. (1940). High proportions of homostyle plants in populations of *Primula vulgaris*. *Nature, 145*, 672–673. doi:10.1038/145672c0

Crosby, J. L. (1949). Selection of an unfavourable gene-complex. *Evolution, 3*(3), 212–230. doi:10.1111/j.1558-5646.1949.tb00022.x

Crosby, J. L. (1959). Outcrossing on homostyle primroses. *Heredity, 13*, 127–131. doi:10.1038/hdy.1959.9

Crosby, J. L. (1960). The use of electronic computation in the study of random fluctuations in rapidly evolving populations. *Philosophical Transactions of the Royal Society B: Biological Sciences, 242*(697), 551–573. doi:10.1098/rstb.1960.0002

Cutter, A. D. (2019). Reproductive transitions in plants and animals: selfing syndrome, sexual selection and speciation. *New Phytologist* 224, 1080–1094.

Curtis, J., & Curtis, C. F. (1985). Homostyle primroses re-visited. I. Variation in time and space. *Heredity, 54*, 227–234. doi:10.1038/hdy.1985.30

Darwin, C. (1876). *The effects of cross and self fertilization in the vegetable kingdom.* London, UK: John Murray.

Darwin, C. (1877). *The different forms of flowers on plants of the same species.* London, UK: John Murray.

David, P., Pujol, B., Viard, F., Castella, V., & Goudet, J. (2007). Reliable selfing rate estimates from imperfect population genetic data. *Molecular Ecology, 16*(12), 2474–2487. doi:10.1111/j.1365-294X.2007.03330.x

de Vos, J. M., Wüest, R. O., & Conti, E. (2014). Small and ugly? Phylogenetic analyses of the "selfing syndrome" reveal complex evolutionary fates of monomorphic primrose flowers. *Evolution, 68*(4), 1042–1057. doi:10.1111/evo.12331

de Vos, J. M., Hughes, C. E., Schneeweiss, G. M., Moore, B. R., & Conti, E. (2014). Heterostyly accelerates diversification *via* reduced extinction in Darwin's primroses. *Philosophical Transactions of the Royal Society B: Biological Sciences, 281*(1784), 20140075. https://doi.org/10.1098/rspb.2014.0075

de Vos, J. M., Keller, B., Isham, S. T., Kelso, S., & Conti, E. (2012). Reproductive implications of herkogamy in homostylous primroses: Variation during anthesis and reproductive assurance in alpine environments. *Functional Ecology, 26*(4), 854–865. doi:10.1111/j.1365-2435.2012.02016.x

de Vos, J. M., Keller, B., Zhang, L. R., Nowak, M. D., & Conti, E. (2018). Mixed mating in homostylous species: Genetic and experimental evidence from an alpine plant with variable herkogamy, *Primula halleri*. *International Journal of Plant Sciences, 179*(2), 87–99. doi:10.1086/695527

Dieringer, D., & Schlötterer, C. (2003). Microsatellite Analyser (MSA): A platform independent analysis tool for large microsatellite data sets. *Molecular Ecology Notes, 3*(1), 167-169. doi:10.1046/j.1471-8286.2003.00351.x

Doyle, J., & Doyle, J. (1987). A rapid DNA isolation procedure for small quantities of fresh leaf tissue. *Phytochemical Bulletin*, *19*, 11–15.

Dulberger, R. (1992). Floral polymorphism and their functional significance in the heterostylous syndrome. In S. C. H. Barrett (Ed.), *Evolution and Function of Heterostyly* (pp. 41–84). Berlin, Germany: Springer-Verlag.

Dwyer, K. G., Berger, M. T., Ahmed, R., Hritzo, M. K., Mcculloch, A. A., Price, M. J., ... Nasrallah, M. E. (2013). Molecular characterization and evolution of self-incompatibility genes in *Arabidopsis thaliana*: The case of the *Sc* haplotype. *Genetics, 193*(3), 985–994. doi:10.1534/genetics.112.146787

Evanno, G., Regnaut, S., & Goudet, J. (2005). Detecting the number of clusters of individuals using the software STRUCTURE: A simulation study. *Molecular Ecology, 14*(8), 2611–2620. doi:10.1111/j.1365-294X.2005.02553.x

Felsenstein, J. (2005). PHYLIP (Phylogeny Inference Package) version 3.6. Distributed by the author. Department of Genome Sciences, University of Washington, Seattle.

Fisher, R. A. (1949). A theoretical system of selection for homostyle *Primula. Sankhyā: The Indian Journal of Statistics, 9*(4), 325–342. doi:10.1002/0471667196.ess1229.pub2

Foxe, J. P., Stift, M., Tedder, A., Haudry, A., Wright, S. .I, & Mable, B. K. (2010). Reconstructing origins of loss of self-incompatibility and selfing in North American Arabidopsis lyrata: A population genetic context. *Evolution,* 64, 3495–3510

Ganders, F. R. (1979). The biology of heterostyly. *New Zealand Journal of Botany, 17*(4), 607–635. doi:10.1080/0028825X.1979.10432574

Gao, H., Williamson, S., & Bustamante, C. D. (2007). A Markov Chain Monte Carlo approach for joint inference of population structure and inbreeding rates from multilocus genotype data. *Genetics, 176*(3), 1635–1651. doi:10.1534/genetics.107.072371

Gilbert, K. J., Andrew, R. L., Bock, D. G., Franklin, M. T., Kane, N. C., Moore, J. -S., ... Vines T. H. (2012). Recommendations for utilizing and reporting population genetic analyses: The reproducibility of genetic clustering using the program STRUCTURE. *Molecular Ecology, 21*(20), 4925–4930. doi:10.1111/j.1365-294X.2012.05754.x

Goodwillie, C. (1999). Multiple origins of self-compatibility in Linanthus section Leptosiphon (Polemoniaceae): Phylogenetic evidence from internal-transcribed-spacer sequence data. *Evolution,* 53, 1387–1395

Goodwillie, C., Kalisz, S., & Eckert, C. G. (2005). The evolutionary enigma of mixed mating systems in plants: Occurrence, theoretical explanations, and empirical evidence. *Annual Review of Ecology, Evolution and Systematics, 36*(1), 47–79. doi:10.1146/annurev.ecolsys.36.091704.175539

Gossmann, T. I., Woolfit, M. & Eyre-Walker, A. (2011). Quantifying the variation in the effective population size within a genome. *Genetics* 189, 1389–1402

Guggisberg, A., Mansion, G., Kelso, S. & Conti, E. (2006). Evolution of biogeographic patterns, ploidy levels, and breeding systems in a diploid-polyploid species complex of Primula. *New Phytologist* 171, 617–632

Hamilton N.E., & Ferry M. (2018). ggtern: Ternary Diagrams using ggplot2. *Journal of Statistical Software*, *87*(3), 1–17. doi:10.18637/jss.v087.c03

Hamrick, J. L., & Godt, M. J. W. (1996). Effects of life history traits on genetic diversity in plant species. *Philosophical Transactions of the Royal Society B: Biological Sciences, 351*(1345), 1291–1298. doi:10.1098/rstb.1996.0112

Hey, J., & Nielsen, R. (2004). Multilocus methods for estimating population sizes, migration rates and divergence time, with applications to the divergence of *Drosophila pseudoobscura* and *D. persimilis*. *Genetics, 167*(2), 747–760. doi:10.1534/genetics.103.024182

Husband, B. C., & Barrett, S. C. H. (1993). Multiple origins of self-fertilization in tristylous *Eichhornia paniculata* (Pontederiaceae): Inferences from style morph and isozyme variation. *Journal of Evolutionary Biology, 6*(4), 591–608. doi:10.1046/j.1420-9101.1993.6040591.x

Huu, C. N., Kappel, C., Keller, B., Sicard, A., Takebayashi, Y., Breuninger, H., ... Lenhard, M. (2016). Presence versus absence of *CYP734A50* underlies the style-length dimorphism in primroses. *Elife, 5*, 1–15. doi:10.7554/eLife.17956

Huu, C. N., Keller, B., Conti, E., Kappel, C., & Lenhard, M. (2020). Supergene evolution via stepwise duplications and neofunctionalization of a floral-organ identity gene. *Proceedings of the National Academy of Science, 117*(37), 23148–23157. doi:10.1073/pnas.2006296117

Jacquemyn, H., Endels, P., Brys, R., Hermy, M., & Woodell, S. R. J. (2009). Biological flora of the British Isles: *Primula vulgaris* Huds. (*P. acaulis* (L.) Hill). *Journal of Ecology, 97*(4), 812–833. doi:10.1111/j.1365-2745.2009.01513.x

Johnson, M. G., Gardner, E. M., Liu, Y., Medina, R., Goffinet, B., Shaw, A. J., ... Wickett, N. J. (2016). HybPiper: Extracting coding sequence and introns for phylogenetics from high-throughput sequencing reads using target enrichment. *Applications in Plant Sciences, 4*(7), 1600016. doi:10.3732/apps.1600016

Jombart, T. (2008). Adegenet: A R package for the multivariate analysis of genetic markers. *Bioinformatics, 24*, 1403–1405. doi:10.1093/bioinformatics/btn129

Kappel, C., Huu, C. N., & Lenhard, M. (2017). A short story gets longer: Recent insights into the molecular basis of heterostyly. *Journal of Experimental Botany, 68*(21-22), 5719–5730. doi:10.1093/jxb/erx387

Keenan, K., Mcginnity, P., Cross, T. F., Crozier, W. W., & Prodöhl, P. A. (2013). DiveRsity: An R package for the estimation and exploration of population genetics parameters and their associated errors. *Methods in Ecology and Evolution, 4*(8), 782–788. doi:10.1111/2041-210X.12067

Keller, B., Ganz, R., Mora-Carrera, E., Nowak, M. D., Theodoridis, S., Koutroumpa, K., ... Conti, E. (2020). Asymmetries of reproductive isolation are reflected in directionalities of hybridization: Integrative evidence on the complexity of species boundaries. *New Phytologist.* doi:10.1111/nph.16849

Keller, B., Thomson, J. D., & Conti, E. (2014). Heterostyly promotes disassortative pollination and reduces sexual interference in Darwin's primroses: Evidence from experimental studies. *Functional Ecology, 28*(6), 1413–1425. doi:10.1111/1365-2435.12274

Kissling, J., & Barrett, S. C. H. (2013). Variation and evolution of herkogamy in *Exochaenium* (Gentianaceae): Implications for the evolution of distyly. *Annals of Botany, 112*(1), 95–102. doi:10.1093/aob/mct097

Kohn, J. R., Graham, S. W., Morton, B., Doyle, J. J., & Barrett, S. C. H. (1996). Reconstruction of the evolution of reproductive characters in Pontederiaceae using phylogenetic evidence from chloroplast DNA restriction-site variation. *Evolution, 50*(4), 1454-1469. doi:1558-5646.1996.tb03919.x

Kopelman, N. M., Mayzel, J., Jakobsson, M., Rosenberg, N. A., & Mayrose, I. (2015). Clumpak: A program for identifying clustering modes and packaging population structure inferences across K. *Molecular Ecology Resources, 15*(5), 1179–1191. doi:10.1111/1755-0998.12387

Kozlov, A. M., Darriba, D., Flouri, T., Morel, B., & Stamatakis, A. (2019). RAxML-NG: A fast, scalable and user-friendly tool for maximum likelihood phylogenetic inference. *Bioinformatics, 35*(21), 4453–4455. doi:10.1093/bioinformatics/btz305

Kumar, S., Stecher, G., Li, M., Knyaz, C., & Tamura, K. (2018). MEGA X: Molecular evolutionary genetics analysis across computing platforms. *Molecular Biology and Evolution, 35*(6), 1547–1549. doi:10.1093/molbev/msy096

Lande, R., & Schemske, D. W. (1985). The evolution of self-fertilization and inbreeding depression in plants. I. Genetic Models. *Evolution, 39*(1), 24–40. doi:10.2307/2408514

Layman, N. C., Fernando, M. T. R., Herlihy, C. R., & Busch, J. W. (2017). Costs of selfing prevent the spread of a self-compatibility mutation that causes reproductive assurance. *Evolution, 71*(4), 884–897. doi:10.1111/evo.13167

Lewis, D., & Jones, D. A. (1992). The genetics of heterostyly. In S. C. H. Barrett (Ed.), *Evolution and Function of Heterostyly* (pp. 129–151). Berlin, Germany: Springer-Verlag.

Li, J., Cocker, J. M., Wright, J., Webster, M. A., McMullan, M., Dyer, S., ... Gilmartin, P. M. (2016). Genetic architecture and evolution of the S locus supergene in *Primula vulgaris*. *Nature Plants, 2*(12), 16188. doi:10.1038/nplants.2016.188

Li, J., Webster, M. A., Wright, J., Cocker, J. M., Smith, M. C., Badakshi, F., ... Gilmartin, P. M. (2015). Integration of genetic and physical maps of the *Primula vulgaris* S locus and localization by chromosome in situ hybridization. *New Phytologist, 208*(1), 137–148. doi:10.1111/nph.13373

Lloyd, D. G., & Webb, C. J. (1992). The selection of heterostyly. In S. C. H. Barrett (Ed.), *Evolution and Function of Heterostyly* (pp. 179–207). Berlin, Germany: Springer-Verlag.

Lopes, J. S., Balding, D., & Beaumont, M. A. (2009). popABC: A program to infer historical demographic parameters. *Bioinformatics, 25*(20), 2747–2749. doi:10.1093/bioinformatics/btp487

Maddison, W. P. and D.R. Maddison. (2019). Mesquite: a modular system for evolutionary analysis. Version 3.61. Retrieved from http://www.mesquiteproject.org

Mast, A. R., Kelso, S., & Conti, E. (2006). Are any primroses (*Primula*) primitively monomorphic? *New Phytologist, 171*(3), 605–616. doi:10.1111/j.1469-8137.2006.01700.x

Mather, K. & Winton, D. DE. (1941). Adaptation and counter-adaptation of the breeding system in Primula. *Annals of Botany* 5, 297–311.

Meirmans, P. G., & Hedrick, P. W. (2011). Assessing population structure: FST and related measures. *Molecular Ecology Resources, 11*(1), 5–18. doi:10.1111/j.1755-0998.2010.02927.x

Morjan, C. L., and Rieseberg, L. H. (2004). How species evolve collectively: Implications of gene flow and selection for the spread of advantageous alleles. *Molecular Ecology, 13*(6), 1341–1356. doi:10.1111/j.1365-294X.2004.02164.x

Ness, R. W., Wright, S. I., & Barrett, S. C. H. (2010). Mating-system variation, demographic history and patterns of nucleotide diversity in the tristylous plant *Eichhornia paniculata. Genetics,* 184(2), 381–392. doi:10.1534/genetics.109.110130

Nielsen, R., & Wakely, J. (2001). Distinguishing migration from isolation: A Markov Chain Monte Carlo approach. *Genetics, 158*(2), 885–896.

Nowak, M. D., Russo, G., Schlapbach, R., Huu, C. N., Lenhard, M., & Conti, E. (2015). The draft genome of *Primula veris* yields insights into the molecular basis of heterostyly. *Genome Biology, 16*(1), 12. doi:10.1186/s13059-014-0567-z

Opedal, Ø. H. (2018). Herkogamy, a principal functional trait of plant reproductive biology. *International Journal of Plant Sciences, 179*(9), 677–687. doi:10.1086/700314

Paradis, E. (2010). Pegas: An R package for population genetics with an integrated-modular approach. *Bioinformatics, 26*(3), 419–420. doi:10.1093/bioinformatics/btp696

Pérez-Barrales, R. & Arroyo, J. (2010). Pollinator shifts and the loss of style polymorphism in Narcissus papyraceus (Amaryllidaceae). *Journal of Evolutionary Biology* 23, 1117–1128

Pérez-Barrales, R., Pino, R., Albaladejo, R. G. & Arroyo, J. (2009). Geographic variation of flower traits in Narcissus papyraceus (Amaryllidaceae): Do pollinators matter? *Journal of Biogeography* 36, 1411–1422

Piper, J. G., & Charlesworth, B. (1986). The evolution of distyly in *Primula vulgaris. Biological Journal of the Linnean Society, 29*(2), 123–137. doi:10.1111/j.1095-8312.1986.tb01827.x

Piper, J. G., Charlesworth, B., & Charlesworth, D. (1984). A high rate of self-fertilization and increased seed fertility on homostyle primroses. *Nature, 310*(5972), 50-51. doi:10.1038/309126a0

Piper, J. G., Charlesworth, B., & Charlesworth, D. (1986). Breeding system evolution in *Primula vulgaris* and the role of reproductive assurance. *Heredity, 56*(2), 207–217. doi:10.1038/hdy.1986.33

Pritchard, J. K., Stephens, M., & Donnelly, P. (2000). Inference of population structure using multilocus genotype data. *Genetics, 155*(2), 945–959. doi:10.1111/j.1471-8286.2007.01758.x

Ralph, P., & Coop, G. (2010). Parallel adaptation: One or many waves of advance of an advantageous allele? *Genetics, 186*(2), 647–668. doi:10.1534/genetics.110.119594

Redelings, B. D., Kumagai, S., Tatarenkov, A., Wang, L., Sakai, A. K., Weller, S. G., ... Uyenoyama, M. K. (2015). A Bayesian approach to inferring rates of selfing and locus-specific mutation. *Genetics, 201*(3), 1171–1188. doi:10.1534/genetics.115.179093

Richards, A. J. (2003). *Primula* (2nd ed.). Portland, USA: Timber Press.

Rigby, R. A., Stasinopoulos, D. M., & Lane, P. W. (2005). Generalized additive models for location, scale and shape. *Applied Statistics, 54*(3), 507–554. doi:10.1111/j.1467-9876.2005.00510.x

Ritland, K. (2002). Extensions of models for the estimation of mating. *Heredity, 88*(4), 221–228. doi:10.1038/sj/hdy/6800029

Rousset, F. (2008). GENEPOP'007: A complete re-implementation of the GENEPOP software for Windows and Linux. *Molecular Ecology Resources, 8*(1), 103–106. doi:10.1111/j.1471-8286.2007.01931.x

Ruiz-Martín, J., Santos-Gally, R., Escudero, M., Midgley, J. J., Pérez-Barrales, R., & Arroyo, J. (2018). Style polymorphism in Linum (Linaceae): a case of Mediterranean parallel evolution? *Plant Biology* 20, 100–111

Schemske, D. W., & Lande, R. (1985). The evolution of self-fertilization and inbreeding depression in plants. II. Empirical observations. *Evolution, 39*(1), 41–52. doi:10.1111/j.1558-5646.1985.tb04078.x

Schoen, D. J., Johnston, M. O., L'Heureux, A.-M., & Marsolais J. V. (1997). Evolutionary history of the mating system in *Amsinckia* (Boraginaceae). *Evolution, 51*(4), 1090–1099. doi:10.1111/j.1558-5646.1997.tb03956.x

Shao, J. W., Wang, H. F., Fang, S. P., Conti, E., Chen, Y. J., & Zhu, H. M. (2019). Intraspecific variation of self-incompatibility in the distylous plant *Primula merrilliana*. *AoB Plants, 11*(3). doi:10.1093/aobpla/plz030

Sharma, V., Hecker, N., Roscito, J. G., Foerster, L., Bjoern, E. L., & Hiller, M. (2018). A genomics approach reveals insights into the importance of gene losses for mammalian adaptations. *Nature Communications* 9, 1–9

Shimizu, K. K., Shimizu-Inatsugi, R., Tsuchimatsu, T., & Purugganan, M. D. (2008). Independent origins of self-compatibility in *Arabidopsis thaliana*. *Molecular Ecology, 17*(2), 704–714. doi:10.1111/j.1365-294X.2007.03605.x

Shimizu, K. K., & Tsuchimatsu, T. (2015). Evolution of selfing: Recurrent patterns in molecular adaptation. *Annual Review of Ecology, Evolution and Systematics, 46*(1), 593–622. doi:10.1146/annurev-ecolsys-112414-054249

Signorell, A., Aho, K., Alfons, A., Anderegg, N., Aragon, A., Arachchige, A., ... Zeileis (2020). DescTools: Tools for Descriptive Statistics. R package version 0.99.39. Retrieved from https://cran.r-project.org/package=DescTools.

Simmons, M. P., & Ochoterena, H. (2000). Gaps as characters in sequence-based phylogenetic analyses. *Systematic Biology, 49*(2), 369–381. doi:10.1093/sysbio/49.2.369

Triest, L., Sierens, T., & Van Rossum, F. (2015). Multiplexing 15 microsatellite loci for European primrose (*Primula vulgaris*). *Conservation Genetic Resources, 7*(1), 279–281. doi:10.1007/s12686-014-0357-7

Valverde, T., & Silvertown, J. (1995). Spatial variation in the seed ecology of a woodland herb (*Primula vulgaris*) in relation to light environment. *Functional Ecology, 9*(6), 942–950. doi:10.2307/2389993

Van Geert, A., Van Rossum, F., & Triest, L. (2010). Do linear landscape elements in farmland act as biological corridors for pollen dispersal? *Journal of Ecology, 98*(1), 178–187. doi:10.1111/j.1365-2745.2009.01600.x

Van Oosterhout, C., Hutchinson, W. F., Wills, D. P. M., & Shipley, P. (2004). MICRO-CHECKER: Software for identifying and correcting genotyping errors in microsatellite data. *Molecular Ecology Notes, 4*(3), 535–538. doi:10.1111/j.1471-8286.2004.00684.x

Vekemans, X., Poux, C., Goubet, P. M. & Castric, V. (2014). The evolution of selfing from outcrossing ancestors in Brassicaceae: What have we learned from variation at the S-locus? *Journal of Evolutionary Biology,* 27, 1372–1385

Voillemot, M., Encinas-Viso, F., & Pannell, J. R. (2019). Rapid loss of self-incompatibility in experimental populations of the perennial outcrossing plant *Linaria cavanillesii*. *Evolution, 73*(5), 913–926. doi:10.1111/evo.13721

Voillemot, M., and Pannell, J. R. (2017). Inbreeding depression is high in a self-incompatible perennial herb population but absent in a self-compatible population showing mixed mating. *Ecology and Evolution,* 7(20), 8535–8544. doi:10.1002/ece3.3354

Weir, B. S., & Cockerham, C. C. (1984). Estimating F-statistics for the analysis of population structure. *Evolution, 38*(6), 1358–1370. doi:10.1111/j.1558-5646.1984.tb05657.x

Woodell, S. R. J. (1960). What pollinates primulas? *New Scientist*, *8*, 568–571.

Wright, S. I., Kalisz, S., & Slotte, T. (2013). Evolutionary consequences of self-fertilization in plants. *Philosophical Transactions of the Royal Society B: Biological Sciences, 280*(1760), 20130133. doi:10.1098/rspb.2013.0133

Yuan, S., Barrett, S. C. H., Duan, T., Qian, X., Shi, M., and Zhang, D. (2017). Ecological correlates and genetic consequences of evolutionary transitions from distyly to homostyly. *Annals of Botany, 120*(5), 775–789. doi:10.1093/aob/mcx09

Yuan, S., Barrett, S.C.H., Li, C., Li, X., Xie, K., and Zhang D. (2018). Genetics of distyly and homostyly in a self-compatible Primula. *Heredity,* 1–10 doi:10.1038/s41437-018-0081-2

Zhang, J. (2000). Rates of conservative and radical nonsynonymous mucleotide substitutions in Mammalian nuclear genes. *Journal of Molecular Evolution*, *50*(1), 56-68. doi:10.1007/s002399910007

Zhao, Z., Luo, Z., Yuan, S., Mei, L., & Zhang, D. (2019). Global transcriptome and gene co-expression network analyses on the development of distyly in *Primula oreodoxa*. *Heredity, 123*(6), 784–794. doi:10.1038/s41437-019-0250-y

Zhong, L., Barrett, S. C. H., Wang, X., Wu, Z., Sun, H., Li, D., & Zhou, W. (2019). Phylogenomic analysis reveals multiple evolutionary origins of selfing from outcrossing in a lineage of heterostylous plants. *New Phytologist, 224*(3), 1290–1303. doi:10.1111/nph.15905

Zhou, W., Barrett, S. C. H., Li, H. D., Wu, Z. K., Wang, X. J., Wang, H., & Li, D. Z. (2017). Phylogeographic insights on the evolutionary breakdown of heterostyly. *New Phytologist, 214*(3), 1368–1380. doi:10.1111/nph.14453

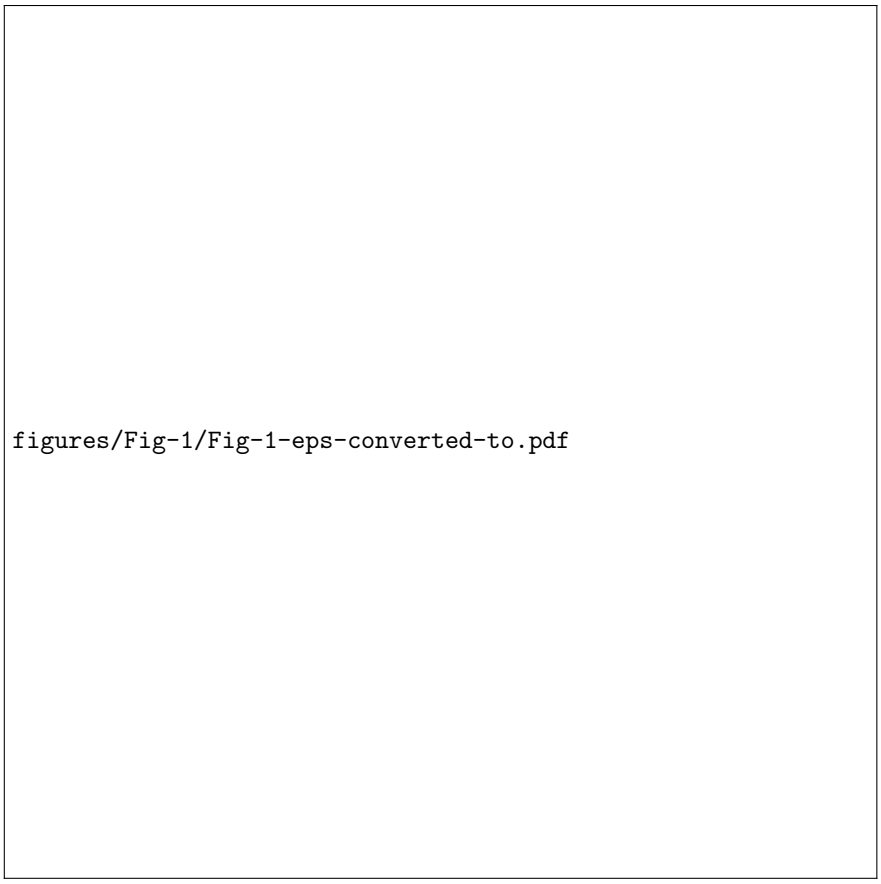

Figure 1: **Figure 1.-** Heterostyly and homostyly in *Primula vulgaris*. Heterostylous floral morphs can be either short-styled (S-morphs) or long-styled (L-morphs). They are characterized by reciprocal placement of male (anthers) and female (stigmas) sexual organs (i.e., reciprocal herkogamy), promoting outcrossing. Additionally, a physiological self-incompatibility mechanism prevents self- and intramorph fertilization. Homostylous floral morphs (H-morphs) are characterized by reduced or no herkogamy and are self-compatible, favoring selfing. Most homostyles have both stigma and anthers at the mouth of the corolla tube (i.e., long-homostyly); short homostyly is rare (not shown). Long-homostyles stem from S-morphs and retain their compatibility type, thus can fertilize only L-morphs. Conversely, S-morphs cannot fertilize long homostyles due to stigma clogging in the latter. Red arrows indicate compatible, likely pollinations between floral morphs. Anthers are represented in yellow and stigmas in green.

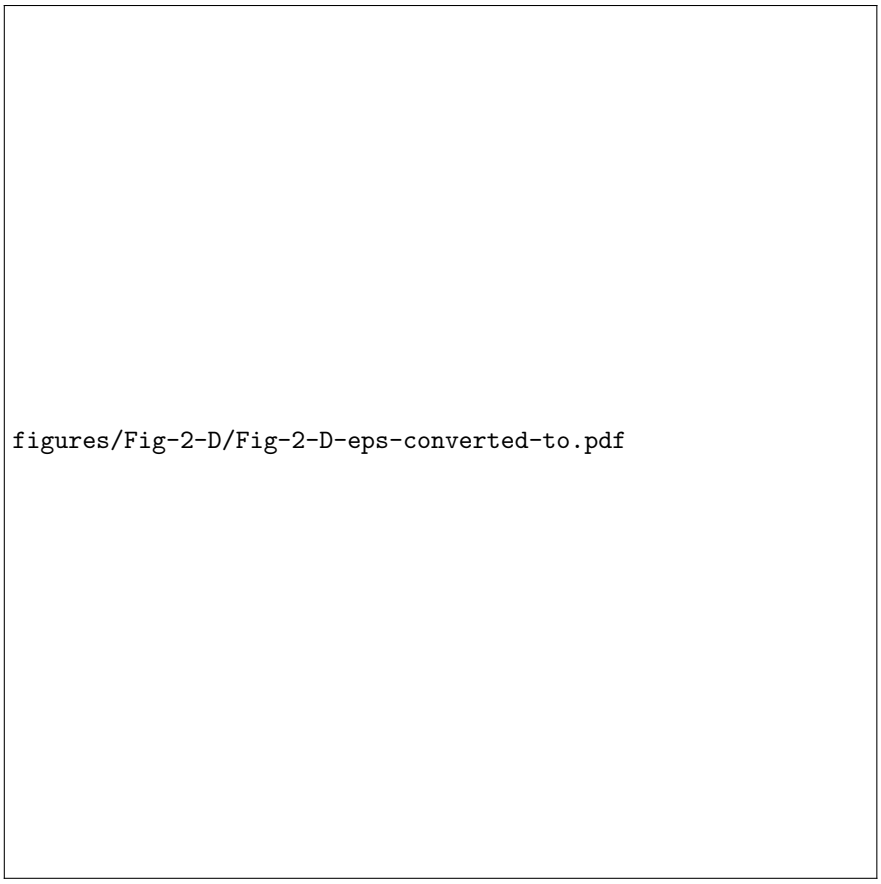

Figure 2: **Figure 2.- A)** Geographic distribution of 22 populations of *Primula vulgaris* from Somerset, England. Pie charts represent intra-population frequencies of long-styled (L; white), short-styled (S; black) and homostylous (H; grey) floral morphs; dimorphic (D) populations consist of L- and S-individuals, except for population D*11, which consists of L- and H-individuals; trimorphic (T) populations consist of L-, S- and H-individuals; the single monomorphic (M) population consists of H-individuals. **B)** Ternary plot representing the frequencies of S-, L- and H-individuals sampled from the same 22 populations. Each vertex of the triangle represents complete population monomorphy for each floral morph; each side of the triangle represents different levels of population dimorphism (bottom: H-morph absent, only L- and S-morphs; left side: S-morph absent, only L- and H-morphs; right side: L-morph absent, only S- and H-morphs); each point inside the triangle represents trimorphic populations; arrow pointing to the base of the triangle represents equal frequencies of S- and L- morphs (i.e., isoplethy); the black dashed line represents the trajectory from isoplethy in distylous populations to complete homostyly observed in the sampled populations; the leftward shift of the line is caused by the greater reduction of S- than L-individuals; the grey dashed line represents the trajectory from isoplethy in distylous populations to complete homostyly with equal reduction of S- vs. L-individuals.

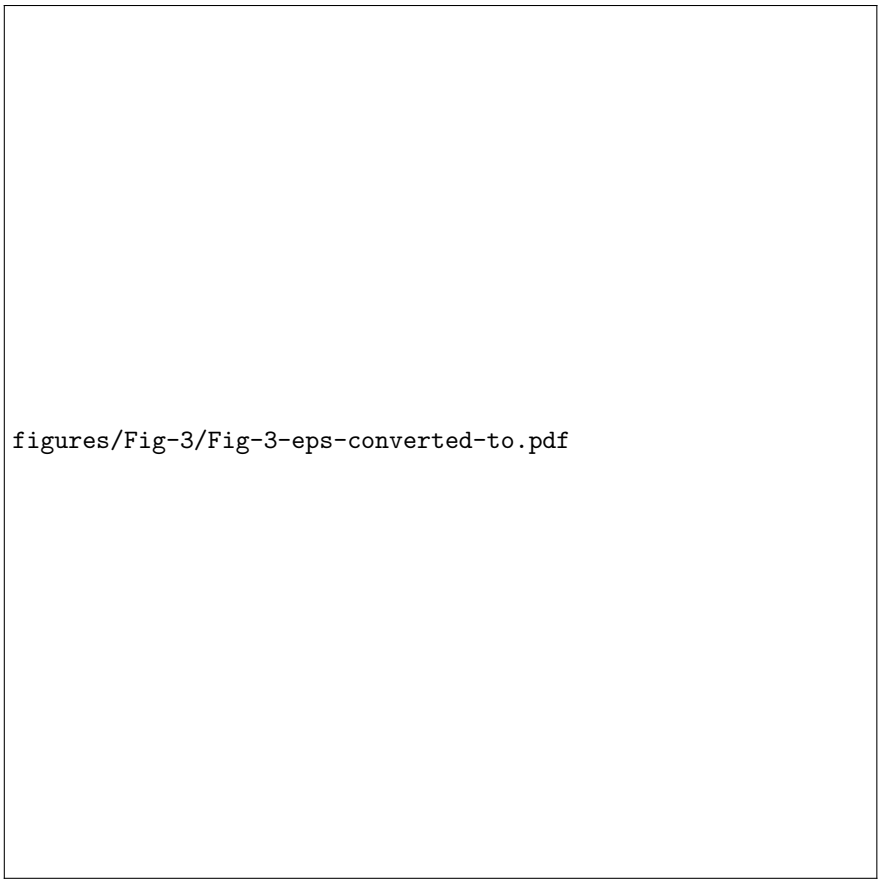

Figure 3: **Figure 3.-** Variation of *CYP?* detected in 44 individuals of *Primula vulgaris* (17 short-styled and 27 homostylous individuals) from ten natural populations sampled for this study, plus two *CYP?* alleles (indicated with *) from two homostylous individuals previously reported as *CYP? S^{LH1}* and S^{LH2} by Li et al. (2016); *CYP?* is a 1587 bp long hemizygous gene that comprises five exons (base-pair lengths of each exon are indicated in parentheses). **A)** Graphical representation of the nine *CYP?* alleles with different types of mutations in *CYP?2–9*: vertical lines, white triangles, and black triangles represent point mutations, deletions, and insertions, respectively, with positions of each mutation reported above each exon; one synonymous, and five nonsynonymous mutations, two deletions, and one insertion were found. **B)** Haplotype network of the nine *CYP?* alleles: each circle (i.e., node in the network) represents a different *CYP?* allele (*CYP?1–9*, listed next to each circle), with circle size proportional to the number of homostylous (grey) and short-styled (black) individuals carrying that allele (reported inside the circle); nodes are connected by solid lines representing the lowest number of mutational steps between alleles, in this case always a single mutational step indicated by a single dash across the line, except for *CYP?-1* and *CYP?-5* connected by two mutational steps; grey dashed lines represent alternative connections among haplotypes with two mutational steps between alleles, indicated by a double dash across the line.

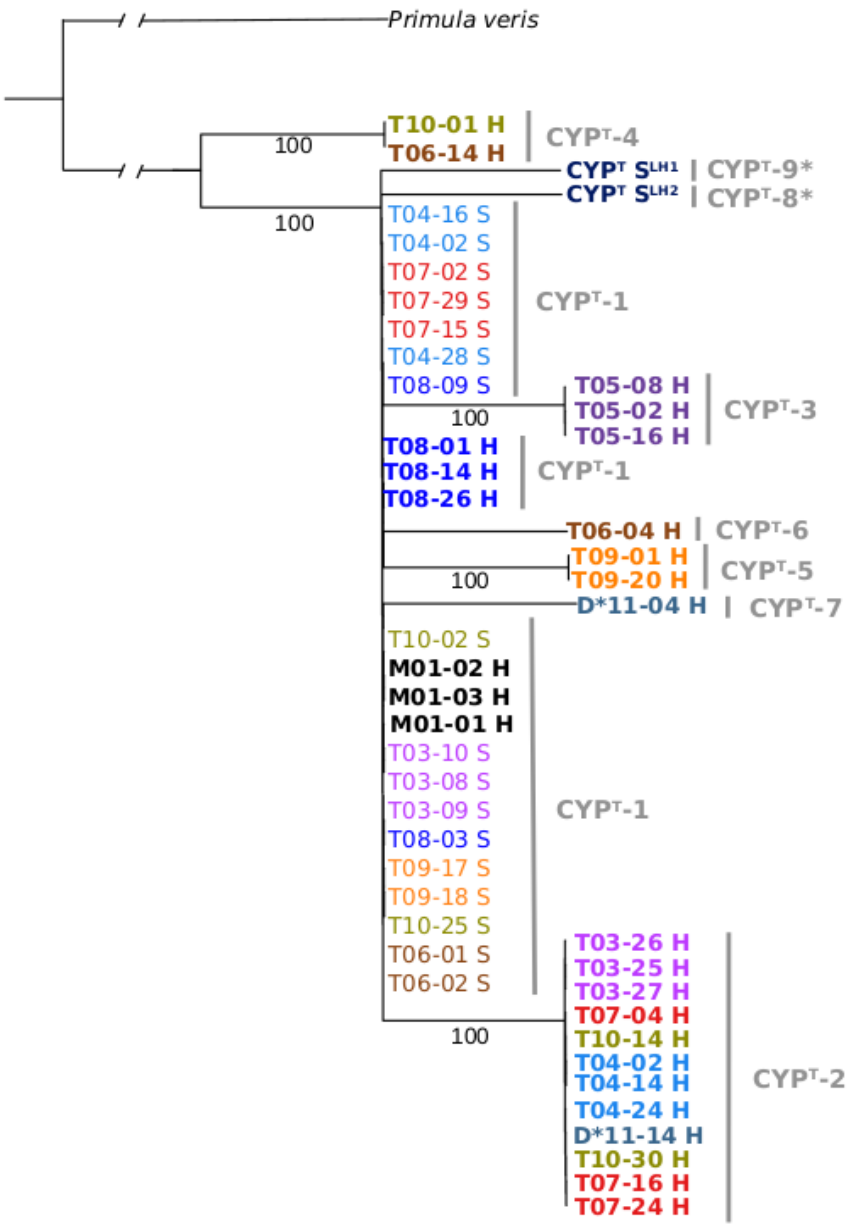

Figure 4: **Figure 4.-** Maximum likelihood tree of *CYP?*sequences from 44 individuals of *Primula vulgaris* (17 short-styled and 27 homostylous, boldfaced) sampled for this study, plus *CYP?* sequences from two homostylous individuals (indicated with *) previously reported as *CYP? S^{LH1}* and *S^{LH2}* (Li et al., 2016), and a *CYP?* sequence from an S-individual of *Primula veris* (GenBank: KX589238) as outgroup. Each accession at the tips is labeled from left to right with population number, individual number, and floral morph type (S and H). Accessions from H-individuals are boldfaced; accessions from the same population have the same color (see also Fig. 2). Bootstrap support values [?] 80 are indicated below to the branches.

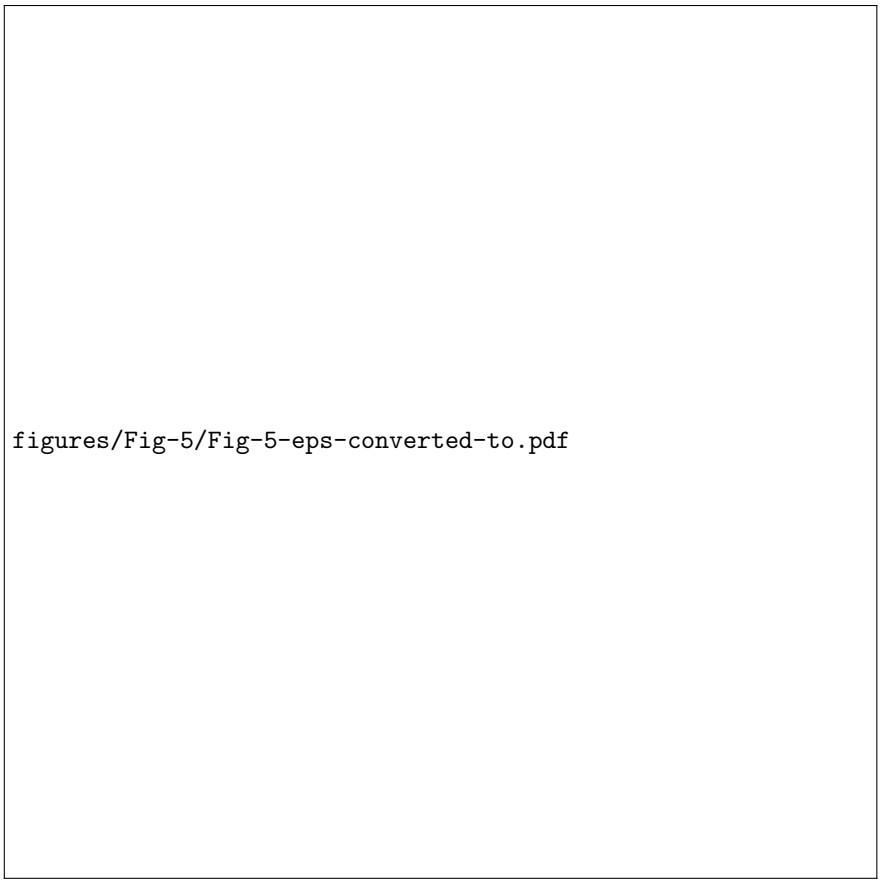

Figure 5: **Figure 5.-** Correlations between population genetic parameters (y axis) and frequency of homostyles (x axis) in 22 natural populations of *Primula vulgaris* inferred from 12 microsatellites: A) Population-level estimates ± 95 % CI of selfing rates based on multilocus linkage disequilibrium (See Methods) and B) Inbreeding coefficient ± 95 % CI.

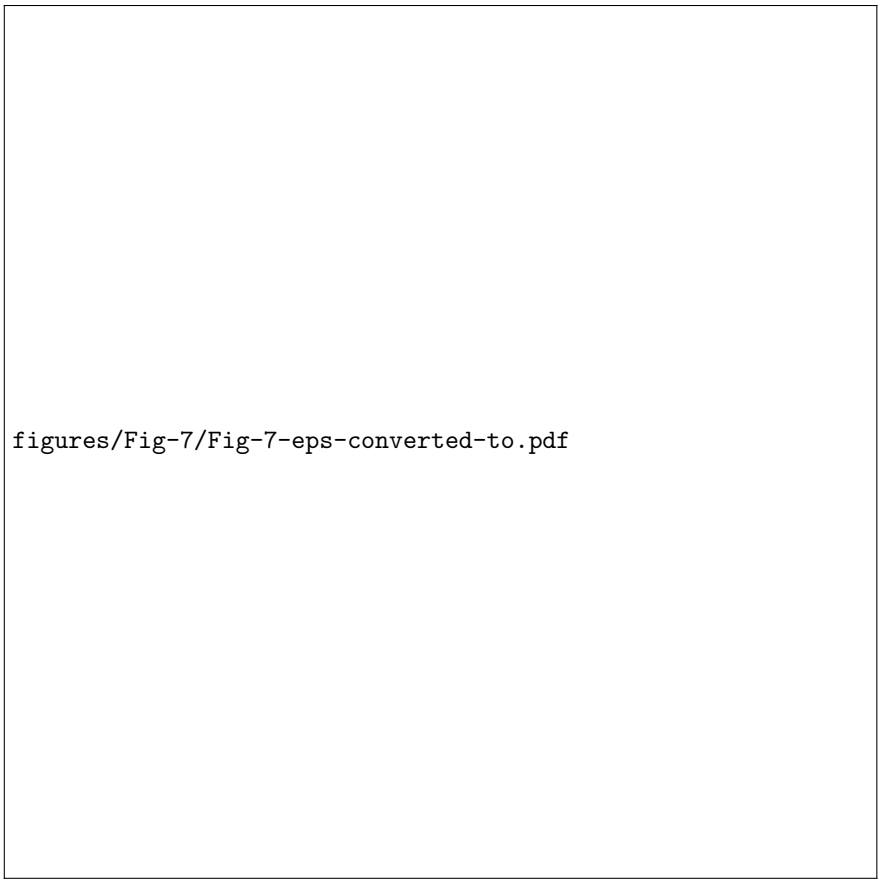

Figure 6: **Figure 6.-** Patterns of genetic differentiation for the 22 natural populations of *Primula vulgaris* . A) Results from InStruct analysis of microsatellites assigning all populations to two genetic clusters (k=2): Optimal number of clusters was selected according to Evanno et al. (2009); B) Plot of the two first PCs from Discriminant Analysis of Principal Components (DAPC) separating population T08 (blue circles) from the rest of the populations

Table 1. Summary data for 22 natural populations of Primula vulgaris sampled in Somerset, England, with floral morph frequencies, levels of inbreeding (Fis), and estimates of population-level selfing rates (s(BES)) inferred using 12 microsatellites. Dimorphic (D) populations consist of long-styled (L) and short-styled (S) morphs, except for population D*11, which consists of LS- and homostylous (HO) morphs; trimorphic (T) populations consist of LS-, SS- and HO-morphs; the single monomorphic (M) population consists of HO-morphs.

Population	Latitude (N), Longitude (E)	Population size	Sample size (morph freq)	Floral Morph			Sample size (pop genetics)	F_{is}	*s(BES)*	*G'st*
				L	S	H				
D01	-2.58°, 51.18°	273	100	0.51	0.49	0	30	0.131	0.180	0.06
D02	-2.63°, 50.98°	~300	96	0.64	0.36	0	30	0.066	0.154	0.07
D03	-2.33°, 50.85°	~500	110	0.44	0.56	0	30	0.071	0.131	0.08
D04	-2.20°, 50.95°	65	65	0.48	0.52	0	24	0.143	0.212	0.08
D05	-2.22°, 51.05°	260	105	0.46	0.54	0	30	0.105	0.318	0.07
D06	-2.49°, 51.23°	~350	101	0.58	0.42	0	30	0.009	0.122	0.09
D07	-2.59°, 51.21°	~250	100	0.58	0.42	0	30	0.149	0.348	0.07
D08	-2.48°, 51.16°	150	94	0.37	0.63	0	29	-0.01	0.222	0.07
D09	-2.49°, 51.05°	~300	100	0.57	0.43	0	29	0.002	0.168	0.07
D10	-2.71°, 51.09°	~500	104	0.52	0.48	0	29	-0.085	0.052	0.08
D*11	-2.42°, 51.13°	58	50	0.34	0	0.66	30	0.065	0.218	0.07
T01	-2.44°, 51.00°	94	94	0.63	0.31	0.06	30	0.117	0.295	0.08
T02	-2.38°, 50.92°	~150	108	0.62	0.32	0.06	24	0.124	0.255	0.07
T03	-2.43°, 51.18°	88	88	0.41	0.38	0.22	30	0.052	0.219	0.07
T04	-2.40°, 51.16°	~200	104	0.36	0.16	0.48	31	0.389	0.529	0.10
T05	-2.25°, 50.95°	20	15	0.33	0.07	0.53	17	0.284	0.473	0.10
T06	-2.56°, 51.14°	79	79	0.41	0.06	0.53	28	0.225	0.422	0.07
T07	-2.30°, 51.08°	103	85	0.29	0.09	0.61	30	0.227	0.394	0.08
T08	-2.58°, 51.09°	161	95	0.36	0.02	0.62	30	0.126	0.314	0.15
T09	-2.55°, 51.05°	87	87	0.33	0.03	0.63	31	0.175	0.318	0.10
T10	-2.42°, 51.10°	~150	82	0.26	0.02	0.72	30	0.251	0.367	0.09
M01	-2.63°, 51.03°	19	19	0	0	1	11	0.272	0.461	0.23
							Mean (± SD)	0.131 (± 0.11)	0.281 (± 0.13)	0.088 (± 0.03)

Fis varies from -1 (heterozygotes excess) to + 1 (homozygotes excess due to inbreeding): values closer to 0 indicate random outcrossing under HWE; population level estimates of selfing rates vary from 0 (maximum outcrossing) to 1 (maximum self-fertilization).

Fis varies from -1 (heterozygotes excess) to + 1 (homozygotes excess due to inbreeding): values closer to 0 indicate random outcrossing under HWE; population level estimates of selfing rates vary from 0 (maximum outcrossing) to 1 (maximum self-fertilization).